# SURFACE STRENGTH VOLT-TIME CHARACTERISTICS OF PROCESSED PRESSBOARD UNDER LIGHTNING, STEEP FRONT AND HIGH FREQUENCY OSCILLATORY IMPULSE VOLTAGES

B y

Yiping Huang

A thesis
presented to the University of Manitoba
in fulfillment of the
thesis requirement for the degree of
Master of Science
in Department of Electrical Engineering

Winnipeg, Manitoba (c)

1990

ISBN 0-315-63271-2

# SURFACE STRENGTH VOLT-TIME CHARACTERISTICS OF PROCESSED PRESSBOARD UNDER LIGHTNING, STEEP FRONT AND HIGH FREQUENCY OSCILLATORY IMPULSE VOLTAGES

BY

YIPING HUANG

A thesis submitted to the Faculty of Graduate Studies of the University of Manitoba in partial fulfillment of the requirements of the degree of

MASTER OF SCIENCE

# ACKNOWLEDEMENTS

The author wishes to express his deep gratitude to his dissertation supervisor Dr. M.R.Raghuveer for his valuable guidance and encouragement during the course of this investigation.

The author also wishes to thank Mr. J. Kendall and Mr. G. Toole for their cooperation and help in constructing the apparatus.

Financial support from Manitoba Hydro which made this investigation possible is also greatly appreciated.

# ABSTRACT

Transformers operating in power systems should have the ability to operate satisfactorily under steep front and oscillatory impulse voltages. In order to assess transformer performance, a knowledge of surface strength of the processed pressboard in mineral oil under steep front and oscillatory impulse voltages is therefore essential. In this study the surface strength volt-time characteristics of cylindrical processed pressboard have been investigated experimentally under lightning , steep front and high frequency oscillatory impulse voltages. Emphasis was placed on the surface strength volt-time characteristics of processed pressboard under steep front impulse voltages with gap lengths of 5 and 10 mm. It is found that the surface breakdown voltage of the processed pressboard does not always decrease with the increase in the breakdown time. An apparent discontinuity of the volt-time characteristics was observed under lightning and steep front impulse voltages and a reduction of surface strength under fast rising voltages was found both at 5 and 10 mm gaps. This abnormal phenomenon is particularly important from the point of view of insulation coordination of power systems and can be possibly explained by the " volt-time area law " or " sweeping action effect " theory.

The surface strength volt-time characteristics of the cylindrical processed pressboard in mineral oil was also conducted under high frequency oscillatory impulse voltages in the range of frequency from 0.2 MHz to 1.15 MHz and

damping factor from 0.65 to 0.8 . It is found that the surface strength is greatest under oscillatory impulse frequency $f = 0.2$ MHz & damping factor $\delta = 0.65$ followed by $f = 0.2$ MHz & $\delta = 0.8$ and $f = 1.15$ & $\delta = 0.8$ for a gap length of 5 mm . These experimental data revealed that the damping factor of the oscillatory impulses has an important influence on the breakdown voltages but the frequency of the oscillatory voltages has little effect on the 50 % surface breakdown values of the processed pressboard.

Finally , the surface breakdown characteristics of processed pressboard in aged oil was investigated under steep front and high frequency oscillatory impulses for the purpose of comparison with data obtained by using fresh unaged oil . It is found that in aged oil , the slope of the volt-time curves are much steeper than that in unaged oil ; also the 50 % surface breakdown voltage decreased almost 25% to 32% comparing to the unaged fresh oil at the same experimental conditions.

# CONTENTS

# LIST OF FIGURES

# CHAPTER 1

# INTRODUCTION

## 1.1 Literature review

Oil-impregnated paper insulation has been used in high voltage power transformers for over fifty years. It has the most lasting characteristics as an insulation system in high voltage apparatus. Recently, several developments concerning ultra-high voltage power apparatus are underway and some prototype ultra-high voltage transformers are being manufactured. Even at the most recent stage,oil-impregnated paper is still the predominant insulation in power transformers and bushings. Some researchers have predicted that Oil-impregnated paper insulation will probably be utilized for more than a century for power transformers [1].

There are many research studies [ 2-13 ] concerning the characteristics of oil-paper insulation systems. These researches have been carried out over a long period throughout the world in order to improve the insulation performance of high voltage power transformers. As early as 1955, Standring and Hughes [2,3] studied the impulse breakdown characteristics of solid and liquid dielectrics in combination. Later Wechsler and Riccitiello [4] investigated the electrical breakdown characteristics of a

parallel solid and liquid dielectric system. They found , under 60 Hz voltages, that breakdown generally occurred in the liquid at or near the liquid-solid interface. The breakdown strength of the combination was as much as 50% lower than the breakdown strength of the oil alone. The researches on dielectric strength of oil impregnated insulation under HVDC stress were carried out by Maier and Vorwerk [5] . In 1981, Kelley and Hebner [6] investigated the electrical breakdown in liquid-solid interface parallel to the field under 60 Hz waveform ;they indicated that, in a carefully prepared system , the breakdown would not necessarily occur at the interface . In addition, it was found that breakdown voltages were not significantly lower for those breakdowns which occurred at the interface than for those which did not. It was noted that if the paper was not dried properly or if many gaseous voids were left in or on the paper, the breakdown regularly occurred at the interface and at a lower voltage . The effect of test geometry, permitivity matching and metal particles on the flashover voltage of oil / solid interfaces under standard impulses was studied by Anker [7]. Recently, cylindrical pressboard with ring shaped electrodes in mineral oil have been considered in [8], it is shown that the presence of the interface lowers the breakdown values. The reduction is 11.9 % and 29.2 % under lightning and switching impulses respectively.

However, all of the above researches have been carried out using conventional voltages such as 60 Hz, dc and standard impulse voltages . As insulation in an operation system is also subjected to non conventional voltage waveforms, non standard voltages have been introduced. In [9] and [10] oil- paper insulation has been considered under a composite voltage waveform consisting both ac and dc components, it is noted that the breakdown voltage decreases with increasing value of the ac component. Tests at extremely low frequency were conducted on oil-paper insulation in [11]. An experimental study of the effect of ripple content of dc

voltage on the surface breakdown strength of processed pressboard in mineral oil has been considered in [12] ; it is found that the ripple has an important effect on the breakdown strength for the gap lengths of 10 mm and 25 mm. The dielectric breakdown of oil-impregnated paper under fast rising impulse voltages has been studied in [ 13 ] , where breakdown times in the submicrosecond range have been obtained.

## 1.2 Steep fronted and oscillatory impulse voltages

The effect of non-standard impulses on interfacial breakdown strength has not been fully investigated especially under fast rising and oscillatory surges.However, the importance and relevance of oil gap insulation under steep front and oscillatory voltages has been discussed by a number of researchers. In this section the phenomena of these impulses will be discussed .

### 1.2.1 Steep front impulses

It has been recognized that a voltage with fast rate of rise, i.e. front times of the order of 0.1 microsecond, may appear in electrical power systems [ 14-17 ]. These steep front voltages may be generated by lightning strikes of the multiple stroke variety. Over half of the lightning flashes to ground have more than one stroke and approximately 5 % of these involve rates of current rise exceeding 100 kA per microsecond [16] . Fast fronts are also generated on the phase conductor during a backflashover from lightning to the tower or shield wire. The process is illustrated

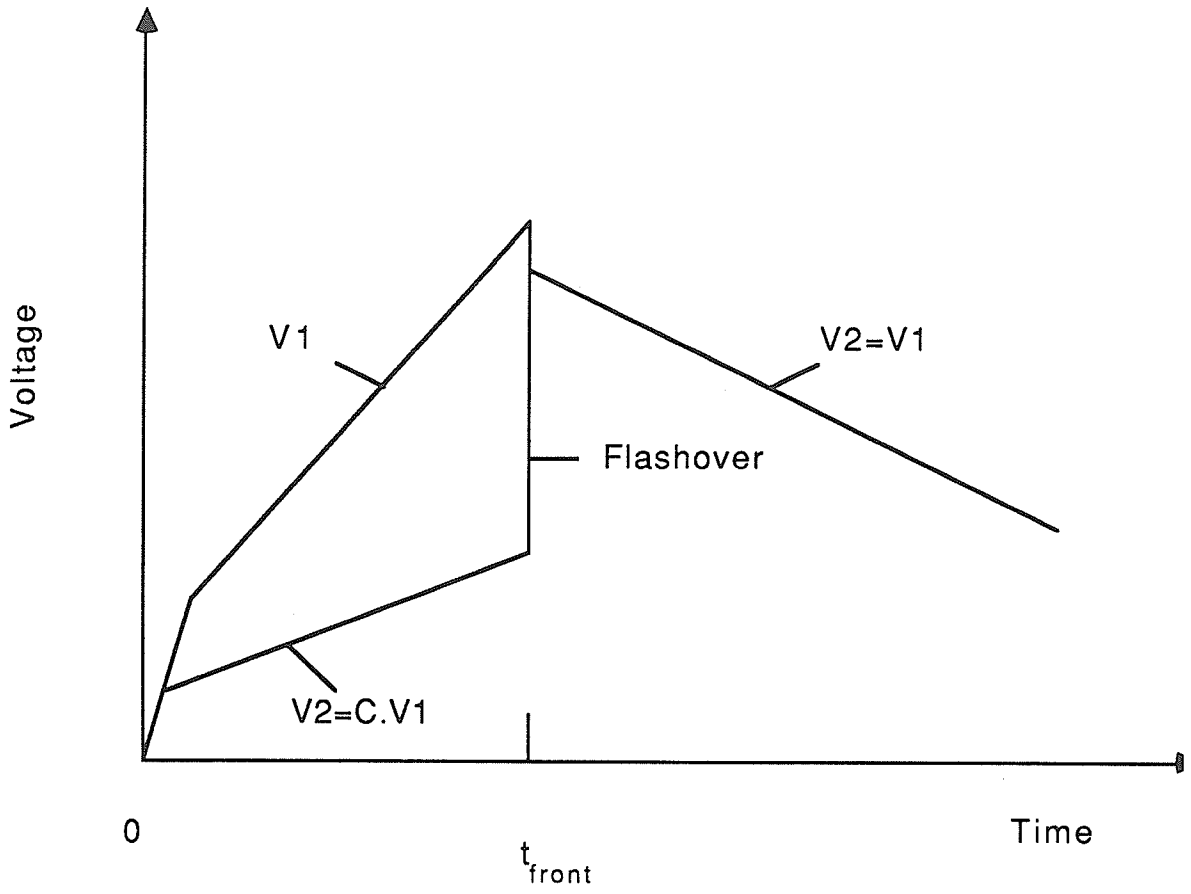


$V1 = V_{shield} = V_{tower}$

$V2 = V_{phase\ conductor}$

C = coupling factor

Figure 1.1: Fast transient on phase conductor generated by backflashover

in Figure 1.1. Following a lightning stroke to the shield wire or tower, the voltage on the tower rises due to the nonzero ground impedance.The phase conductor voltage also rises as it is electrostatically coupled to the tower .When the withstand voltage of the insulation string is exceeded, flashover occurs between the tower and the phase conductor which results in an abrupt increase in the phase conductor voltage. Note that this mechanism does not depend upon the front time of the lightning stroke. Another possible source of fast front pulse is an atmospheric nuclear explosion . Current pulses of the order of tens of kiloamperes rising in approximately 10 nanoseconds may be induced in power transmission lines. In contrast to lightning generated pulses, these pulses appear almost simultaneously throughout a line and are more difficult to protect against. Research has showed that transformers may fail under fast rising voltage [13-17]. Thus the examination of the behavior of extra high voltage insulation under steep front impulses is important from the point of view of coordination of insulation strengths. There are few published data available on the oil-paper insulation under steep front impulse voltages. However there have been a number of studies on the insulation characteristics under steep front impulses in SF6 gas insulation systems [18-20].

### 1.2.2 Oscillatory impulses

Due to the presence of capacitance and inductance in any systems, impulse voltages are generally oscillatory and of a complex nature. Thus power transformers should have the ability to operate safely under oscillatory voltages. The waveform of such voltages is usually varied with different frequencies and damping factors. Oscillatory voltages are produced due to various reasons , including lightning strokes, line faults, line switching etc. The oscillation frequency produced by

lightning is of the order of several hundred Hertz and that produced by line fault for line switching is 1 to 50 kHz [21]. The frequency of the oscillation caused by the potential oscillating inside the winding is of the order of 10 to 200 kHz [22] . An oscillatory impulse can also be caused by flashovers or isolator switching in SF6 gas insulated substations.Frequencies up to the mega Hertz range have been measured [20]. The breakdown behavior with extremely high frequencies is therefore of special interest.

The breakdown characteristics of an oil gap under high frequency oscillatory impulse voltages has been the subject of several studies. The breakdown behavior of transformer oil was investigated with various damping factors, frequencies, and polarities in [ 21-25 ]. However, no data has been reported in the literature on characteristics of the oil-impregnated paper insulation under applied oscillatory impulse voltage. Therefore, it occurred to the author that research should be carried out on the surface strength voltage-time characteristics of processed pressboard under high frequency oscillatory impulses.

## 1.3 Present investigation

Review of previous work showed that investigations on the volt-time characteristics of the oil-impregnated paper insulation were very limited especially under steep front and damped oscillatory impulse voltages. In order to enable the complete evaluation of existing insulation systems , a study of the breakdown characteristics of the oil-impregnated paper insulation under these impulses has been carried out.

The main objective of this investigation is to gain valuable information

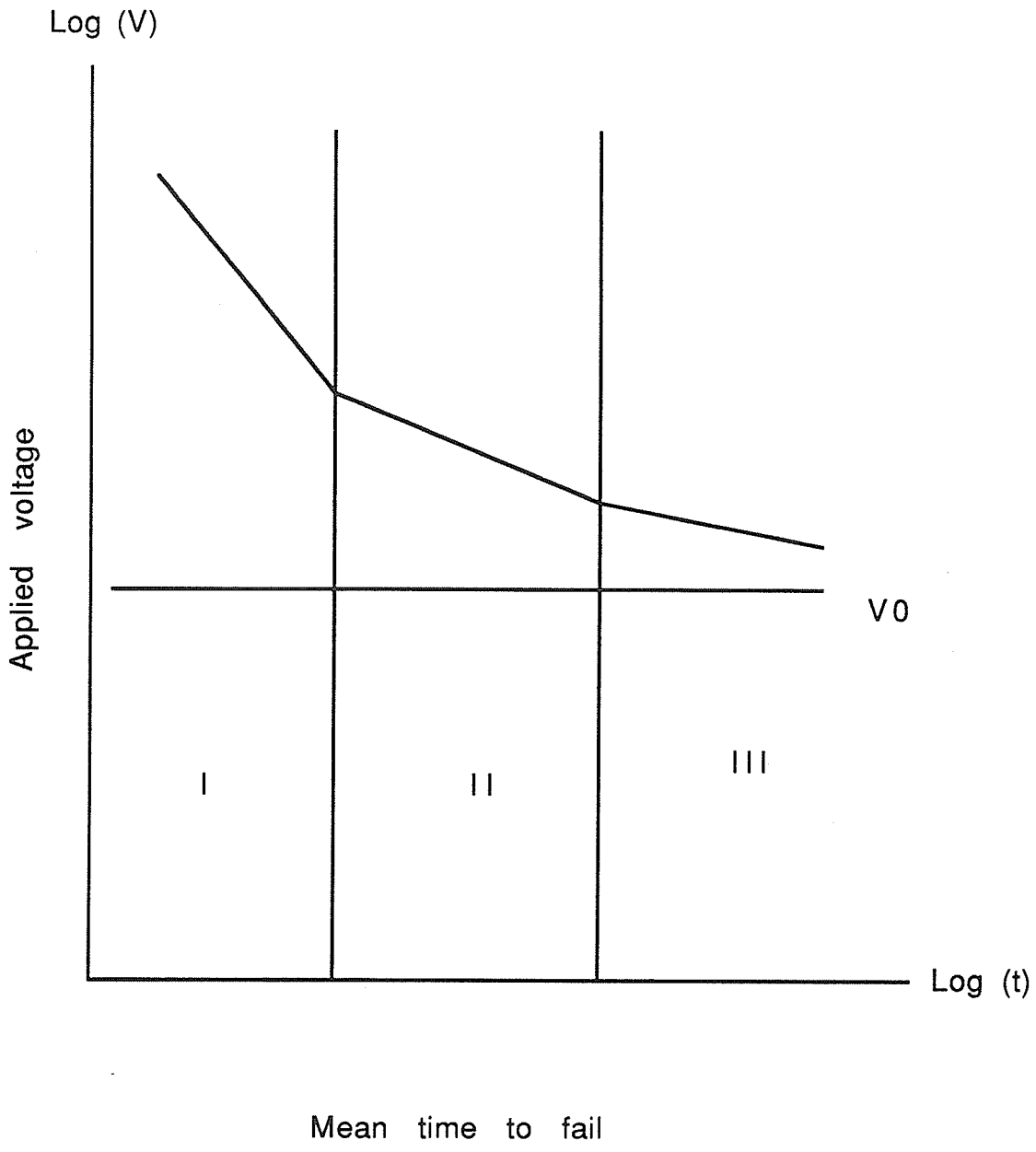


I: 1st region, II: 2nd region, III: 3rd region V0: Threshold voltage

Figure 1.2: General characteristics of voltage-life-time curves [26]

on the breakdown characteristics of processed pressboard under lightning, steep front and damped high frequency oscillatory impulse voltages in unaged fresh oil. Since electrical apparatus operating in the field deteriorate slowly and will finally become unstable, hence the investigation on the surface strength of processed pressboard was extended to include aged oil procured from transformer operating in the field. A typical voltage-life-time characteristics of electrical insulation systems is shown in Figure 1.2 [ 26] , where t is the mean time to failure, and V is the applied stress. In this figure, there are three regions in the volt-life-time curve and a linear relationship between log(t) and log(V) in each region.

The thesis is organized in the following manner, the test equipment and impregnation procedures are described in chapter 2 . Chapter 3 presents methods to generate the waveforms used in this investigation , including lightning, steep front and damped high frequency oscillatory voltage impulses , and the experimental techniques. Chapter 4 presents the experimental results and their discussions. The volt-time characteristics under standard lightning, steep front impulses (with minimum fronted time of 0.15 microsecond) and oscillatory impulse with frequency in the range 0.2 to 1.15 MHz & damping factor in the range 0.65 to 0.8 are included in this chapter for gap lengths of 5 mm and 10 mm. The following chapter, Chapter 5, presents some theoretical considerations. In the final chapter, Chapter 6, conclusions are drawn and a discussion included concerning the significance of the results are obtained.

# CHAPTER 2

# TEST EQUIPMENT AND IMPREGATION PROCEDURE

## 2.1 Test equipment

The main components of the test equipment consist of test chamber, specimens, mineral oil and vacuum system.

### 2.1.1 Test chamber

The investigations were carried out in a glass chamber , shown in Figure 2.1, of height 500 mm and an inner diameter of 300 mm with wall thickness 7 mm. The chamber was sealed at both ends with silicone " o " rings against chromed stainless steel plates. Provision was made for surrounding the walls of the test chamber with an insulating jacket containing a heating element to enable the conduct of tests at elevated temperatures. The volume of the glass chamber is 35 liters.

### 2.2.2 Test specimens and electrode arrangement

Ring shaped brass electrode of outer diameter 199.2 mm, inner diameter

157. 0 mm and of width 10.0 mm were fitted snugly around the cylindrical pressboard sample of wall thickness 2.3 mm , inner diameter 152.4 mm and length about 160 mm. The pressboard was a precompressed grade known as type TIV and was supplied in cylindrical form by the E.H.V. Weidmann company. The material is normally used as insulating material in power transformers.

As seen in Figure 2.2, six electrodes could be assembled on each pressboard specimen to yield 5 gaps of 5 or 10 mm. The gap spacing was ensured by providing three cylindrical Teflon spacers of the same length, which were located symmetrically at the outer edge of the electrodes. The high voltage electrode was connected to the top plate of the glass chamber and the low voltage electrode was fixed to the bottom stainless steel plate. The assembly consisting of the electrodes and spacers was held in place securely by means of permali holders. Considerable care was exercised to ensure that the spacers were symmetrically situated for all the gaps tested. Before assembly each electrode, spacer and holders were washed thoroughly with methanol.

### 2.1.3 Vacuum system

The test chamber was evacuated by a single stage rotary pump with nominal pumping speed 600 l / min and end vacuum $10^{-3}$ Torr. Vacuum valves and gauges were connected as shown in Figure 2.3. The leakage rate characteristic of the system was determined with valves 2, 3, and 4 closed at temperature of 25°C in the pressure range of $10^{-1}$ torr.

The leakage rate was determined using

$$N = V \frac{\Delta P}{\Delta t} \qquad (2.1)$$

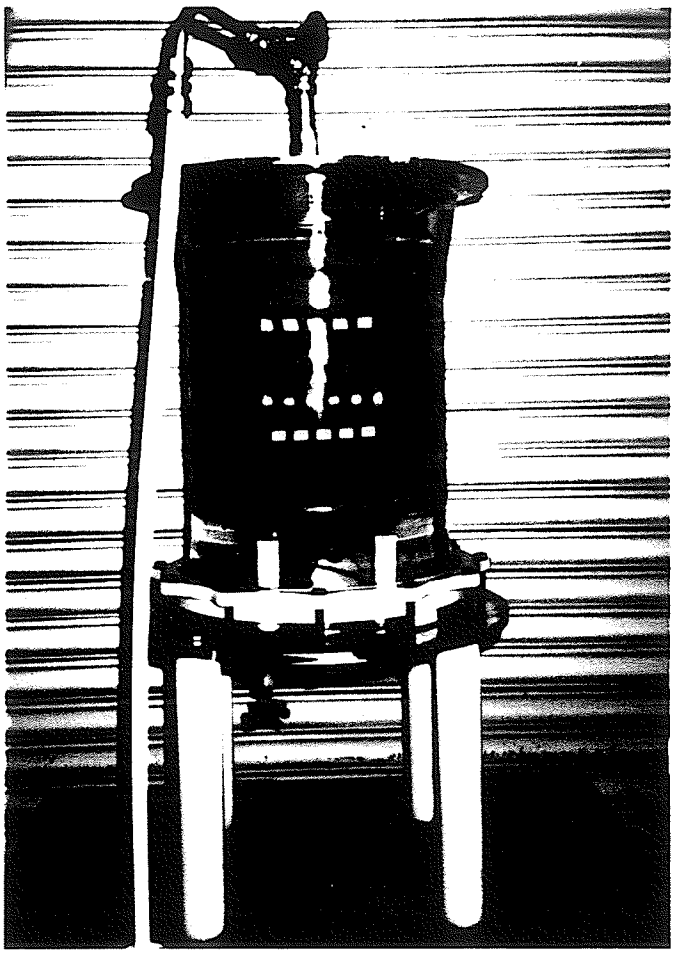

Figure 2.1: Test chamber with test specimen

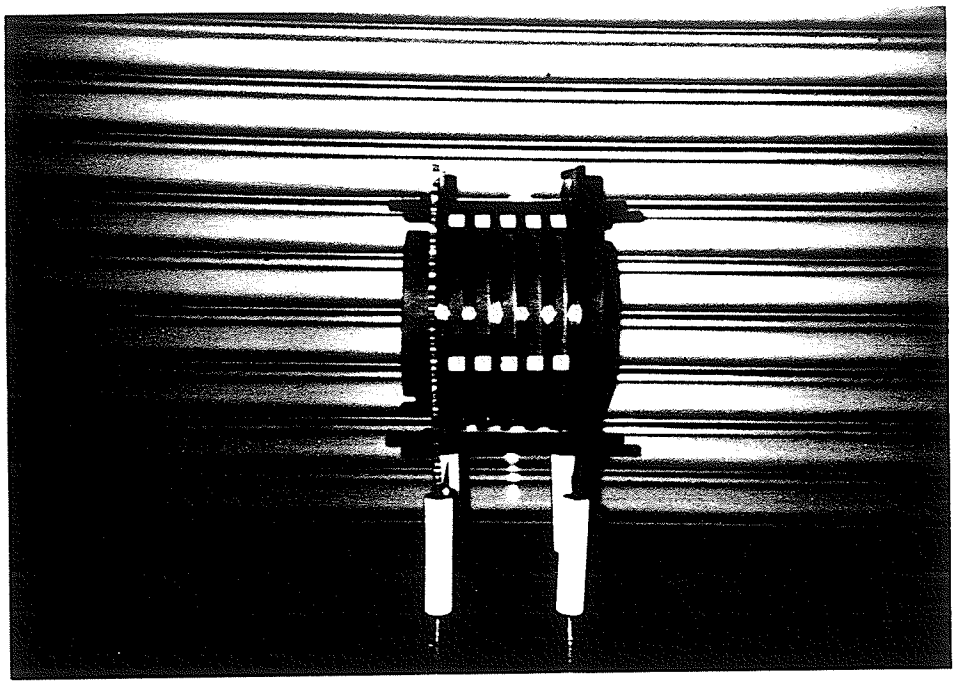

Figure 2.2 Test sample and electrode arrangement

Where N = leakage rate in torr l / s

V = volume of system ( 35 l )

$\Delta P$ = Increase in pressure due to evaporation of moisture and real leakage.

Evacuation of the vessel continued until the leakage rate, N, settled to a steady value. At this point the increase in pressure in the vessel with the pump disconnected is solely due to real leakage. The system leakage rate characteristics are shown in Figure 3.4. From the curve the leakage rate can be determined, the steady state leakage rate was approximately equal to $10^{-2}$ Torr l / s. Under this condition the amount of moisture by weight remaining in the paper is less than 0.5 percent.[27].

### 2.1.4 Impregnating oil

The impregnating insulants used were refined mineral oil, VOLTESSO 35, and aged mineral oil procured from Dorsey T22 converter transformer operating in the Manitoba Hydro systems since 1975.

The mineral oil was degassed and dried in an oil storage tank before impregnation. There are 3 stages in this procedure lasting a total 72 hours. In the first stage, 10 liters of oil was degassed at a temperature of 30°C and under a vacuum of $10^{-1}$ Torr for a 24 hour period. At the end of this period an additional 10 liters was introduced in the storage tank and the second degassing stage commenced which lasted 24 hours. Finally, 10 more liters was introduced in the tank and processed in a similar manner. After these 3 stages , the 30 liters oil

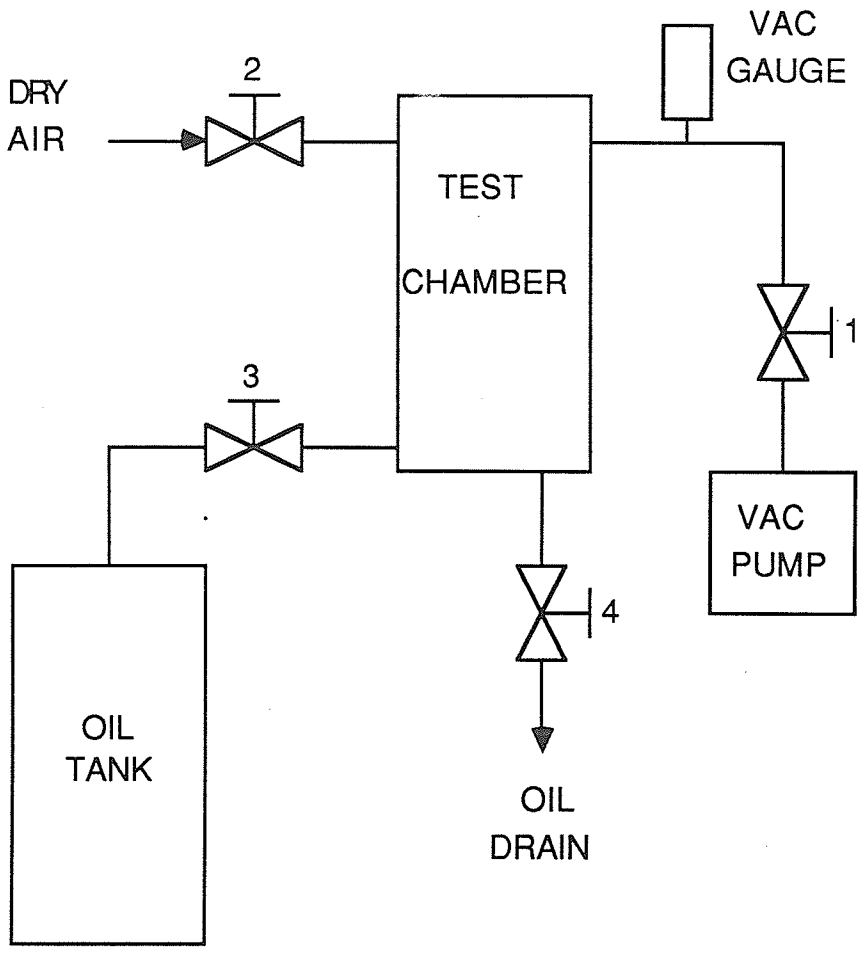


Figure 2.3: Block diagram of vacuum system

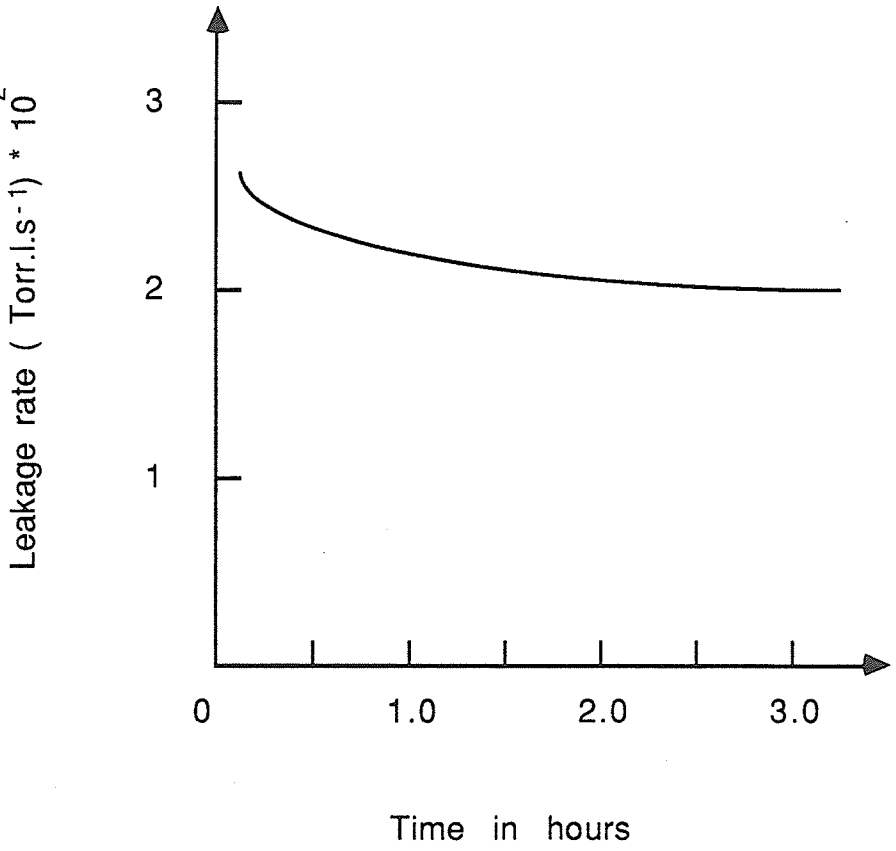


Figure 2.4: System leakage rate characteristics

was introduced from the oil storage tank into the test chamber which needed 6 hours. Then the impregnated sample was ready for testing which usually took two days. Thus, it takes almost one week for preparation and testing one sample.

In this investigation, both the refined oil and aged oil were tested for water content and loss factor. The dissipation factor of the unprocessed oil was 0.35 % at room temperature and 0.3 % at 100°C. The dissipation factor of the processed oil at room temperature and 100°C was measured to be 0.202% and 0.262 % respectively. The dissipation factor was measured in a concentric cylindrical test cell with radial electrodes spaced 0.425 mm using a low voltage Schering bridge at a frequency of 1 kHz. In these tests the oil was stressed at an average value of 100 V /mm [12]. The moisture content of processed oil was less

TABLE 2.1

| Item | New oil | Aged oil |
|---|---|---|
| Colour | 0.5 | 2.0 |
| Neutralization | 0.5 mg KOH/g | 0.02 mg KOH/g |
| Interfacial tension | 45 mN/m | 31.8 mN/m |
| Dissolved water | < 10 ppm | 6 ppm |
| Dissipation factor at 100 °C | 0.262% | 0.74% |

than 10 ppm.The dissipation factor of the aged oil was 0.74 % at 100°C and the moisture content of the aged oil was less than 7 ppm. It can be seen that the dissipation factor of aged oil is much larger than that of the new oil. The characteristics of the new oil are compared with those of Table 2.1.

## 2.2 Impregnation procedure

To develop an acceptable drying technique, four procedures were initially tried out using circular samples of TIV pressboard of thickness 2.3 mm and diameter 150 mm. In the first procedure the sample was inserted in a test chamber and evacuated at room temperature for a 24 hour period. In the second procedure the sample was preheated in an oven for 24 hour at 100° C prior to vacuum drying at room temperature for 24 hours . The third and fourth procedures were similar to the first and second procedures respectively except that vacuum drying was carried out at 70°C. In all cases the end vacuum was between 0.3 and $0.5 \times 10^{-2}$ Torr. The dissipation factor of the samples was monitored by means of low voltage Schering bridge at 1 kHz.

Figure 2.5 shows the variation of dissipation factor with time of evacuation for the four procedures . As expected the dissipation factor decreased with vacuum application time. Also, the pressboard sample subject to the fourth drying procedure showed the lowest dissipation factor.

Based upon the above results the following drying and impregnating procedure was adopted:

The assembly consisting of sample and electrodes was placed in an oven and preheated

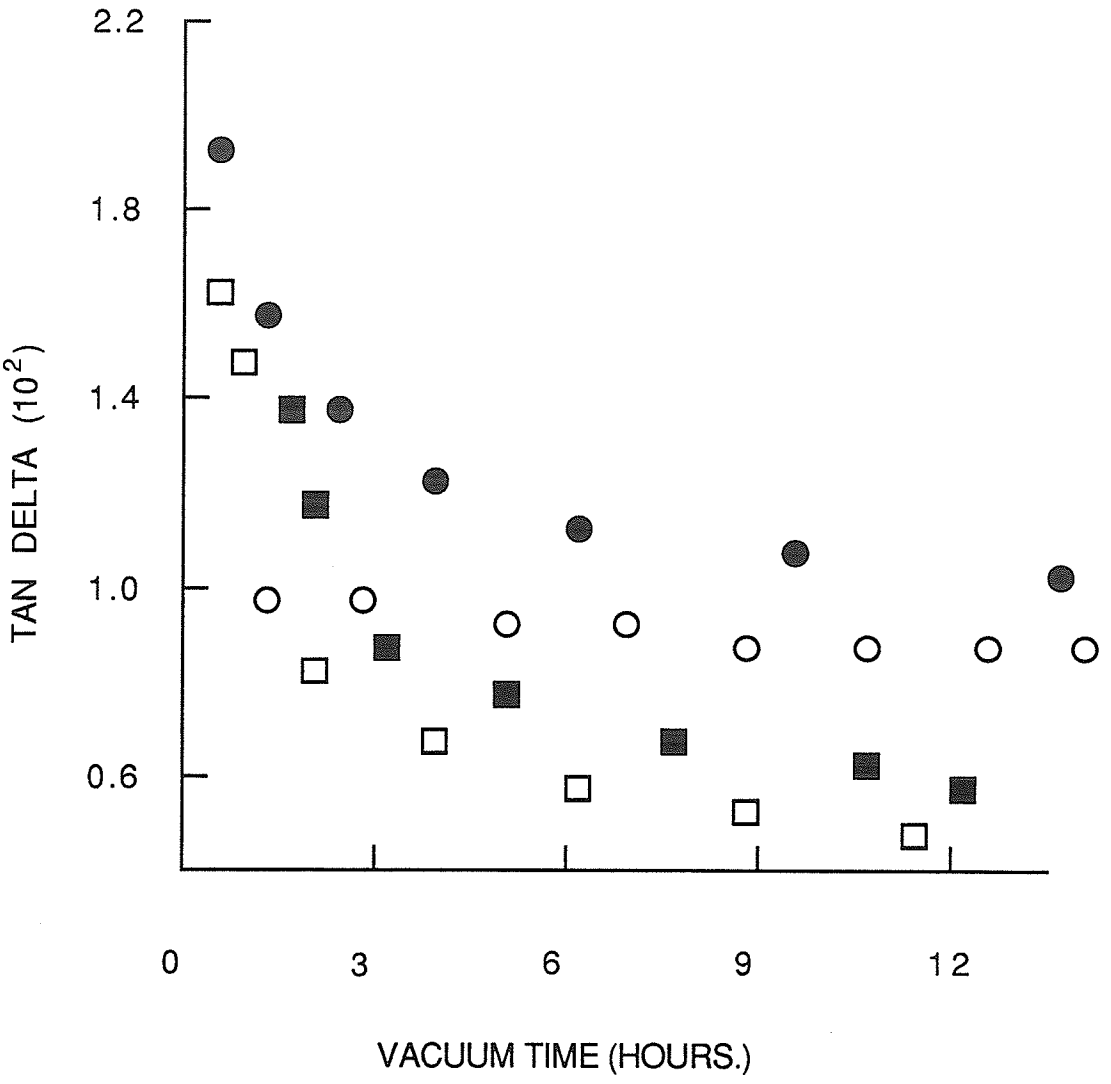


● Sample evacuated in vessel at room temp. without preheat.

○ Sample evacuated in vessel at room temp. after preheat for 24 hours.

■ Sample evacuated in vessel at 70° C without preheat

□ Sample evacuated in vessel at 70° C after preheat for 24 hours

Figure 2.5 : Variation of dissipation factor with evacuation time for the four procedures considered [12 ]

for 24 hours at a temperature of 100°C. After preheating the assembly was transferred into the test chamber for vacuum drying for further period of 24 hours at a temperature of 70°C. The end vacuum was between 0.3 and 0.5 $10^{-2}$ Torr. The sample was then vacuum impregnated slowly under a vacuum of less than $10^{-1}$ Torr. with oil at room temperature. This process took approximately 3 hour to complete at the end of which the test chamber was filled with approximately 30 liters of oil. Vacuum was maintained inside the chamber for at least a further 3 hour period until no bubbles could be observed. Pressure was then returned to atmospheric value by admitting air into the chamber through a dessicator.

# CHAPTER 3

# TEST CIRCUITS AND EXPERIMENTAL TECHIQUES

## 3.1 Circuit to generate lightning impulse

Standard lightning impulse voltage was generated by an 8 stage, 800 kV, 100 kV/stage, 10 kJ, impulse generator. With the aid of appropriate waveshaping resistors it was possible to generate a waveshape of 1.47/47 μs. The breakdown voltages and times to breakdown were measured using a mixed parallel RC Haefly impulse voltage divider connected to a type 466 tektronix storage oscilloscope . The breakdown voltages measured were the peak voltage magnitudes.

The circuit used to generate the lightning impulse is shown in Figure 3.1. With this circuit arrangement a standard lightning impulse can be obtained. Figure 3.2 and 3.3 shows the typical waveforms of the lightning impulse.

## 3.2 Circuit to Generate steep front impulse

The circuits used to generate the steep front impulses is shown in Figure 3.4. Figure 3.5 and 3.6 shows typical waveshapes of the steep front impulse voltages. The impulse generator described in 3.1 was used as a power supply for the circuit.

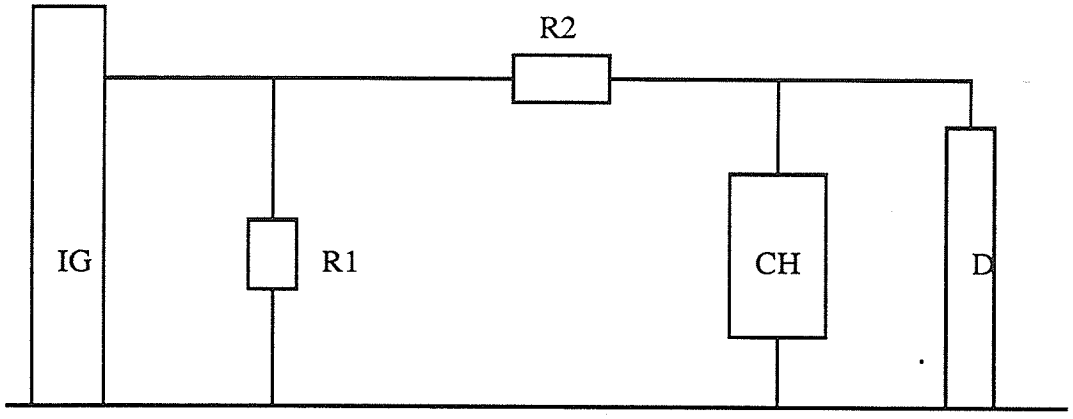


Figure 3.1: Lightning impulse generating circuit. IG-impulse generator; CH-test chamber; D-voltage divider; R1,R2-noninductive resistors.
R1= 1643.6 Ω ; R2= 507.7 Ω

As shown in the figure, in order to lessen the effect of the impulse generator on the output steep front impulse a large value resistor was chosen for R1. The desired impulse waveshape was obtained by choosing appropriate resistances for R2 and R3 in the circuits. With this arrangement a steep front impulse of 0.15/15 us can obtained.

With the front time range to be used in this investigation, it was immediately realized that measurement would be a problem since the mixed parallel RC impulse voltage divider is not suitable for the measurement of steep front impulses because of

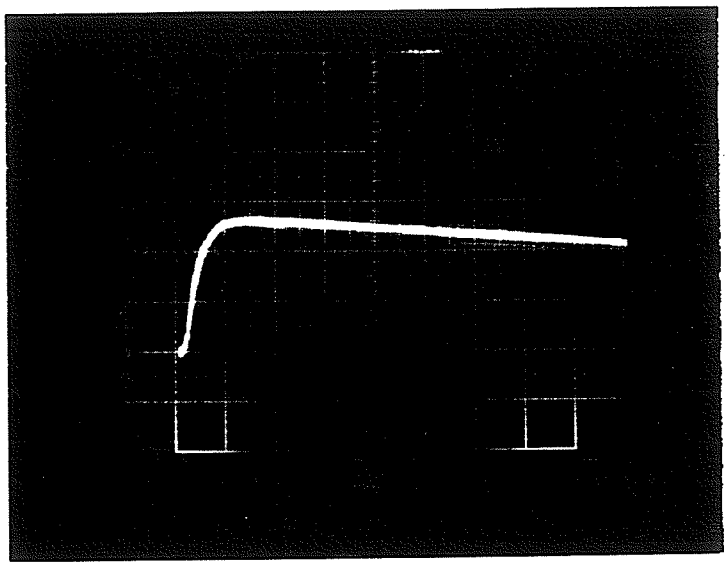

Figure 3.2: Lightning impulse wavefront oscillogram: positive polarity.
Time: 2 μs/cm ; Volt: 10 V/cm

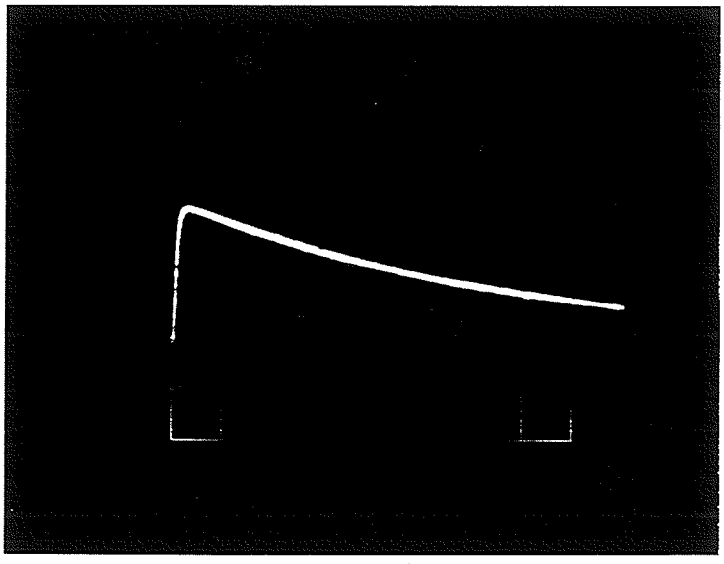

Figure 3.3: Lightning impulse wavefront oscillogram: positive polarity.
Time: 10 μs/cm ; Volt: 10 V/cm

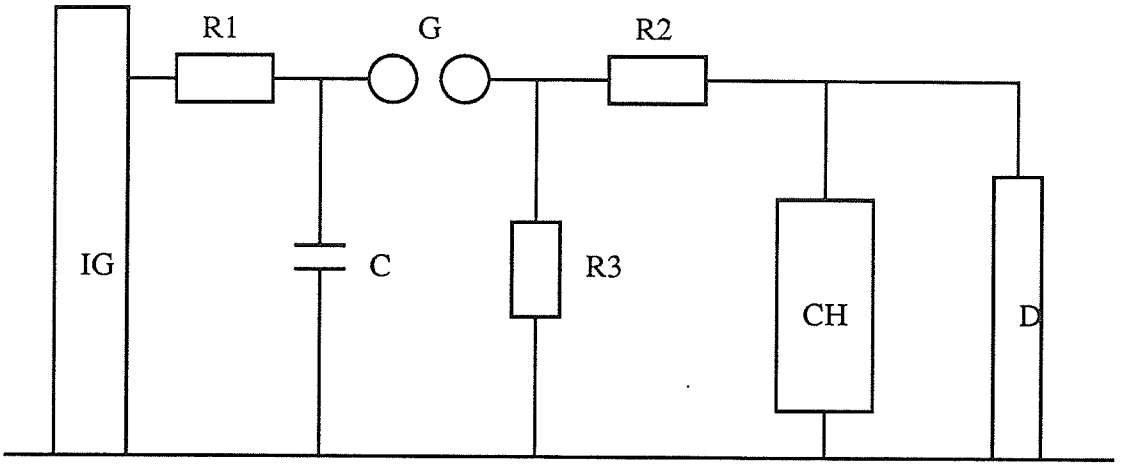


Figure 3.4: Steep front impulse generating circuit. IG-impulse generator; CH-test chamber; D-voltage divider; R1,R2,R3-noninductive resistors; C-capacitor, G-sphere gap
R1= 35 kΩ; R2= 526
R3=5000 Ω; C= 250 pF

their slow unit step responses. Therefore a compact resistor divider with a fast step response was employed.The unit step response time of the compact resistor divider is 8 ns [28]. Hence, with this divider, the measuring error can be greatly reduced.

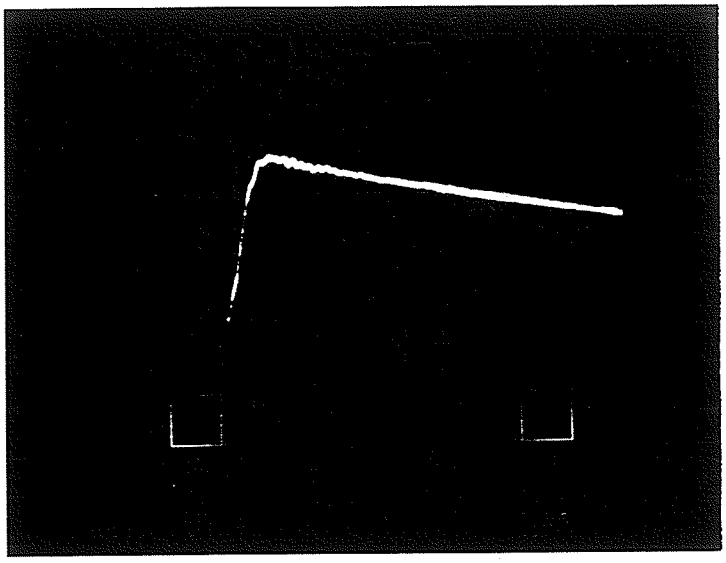

Figure 3.5. Steep front impulse wavefront oscillogram: positive polarity.
Time: 0.2 μs/cm; Volt: 10 V/cm

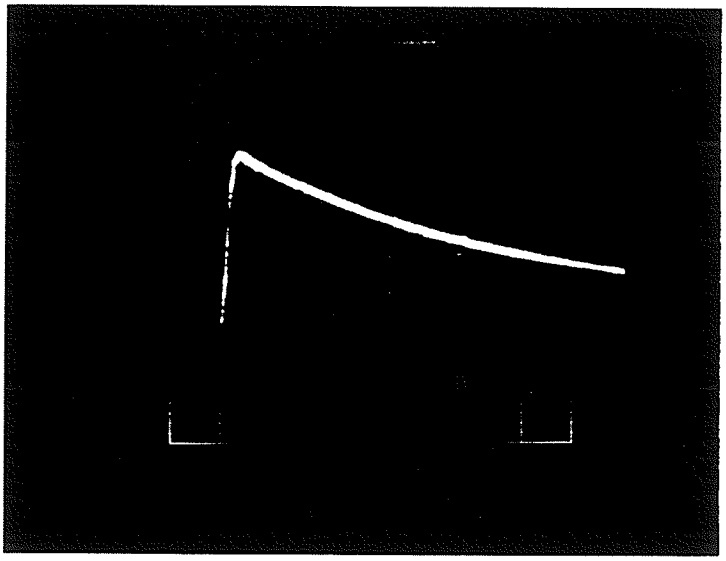

Figure 3.6: Steep front impulse wavefront oscillogram: positive polarity.
Time: 0.5 μs/cm ; Volt: 10 V/cm

## 3.3 Circuits to generate high frequency Oscillatory impulses

Because there are different capacitances and inductances in different systems, the oscillatory impulse voltages in actual power systems are generally of a complex nature. In order to assess the insulation of the systems sufficiently, two different high frequency oscillatory impulse circuits with various frequency and damping factors were set up.

### 3.3.1 Bidirectional oscillatory impulse circuit

The circuit used to generate the bidirectional damped oscillatory impulse is shown in Figure 3.7. The oscillation frequency and the damping factor are varied by changing the inductance L and the series resistance R.

The terminal voltage V(t) across the test chamber is given by

$$V(t) = \frac{E}{\beta\sqrt{LC}} e^{-\alpha t} \cos(\omega t + \theta) \qquad (3.1)$$

Where E is the charging voltage of the capacitor C and

$$\alpha = \frac{R1}{2L}$$

$$\beta = \sqrt{\frac{R1}{LC} - \frac{R1}{4L^2}}$$

$$\theta = \frac{\pi}{2} - \tan^{-1}\left(\frac{\beta}{\alpha}\right)$$

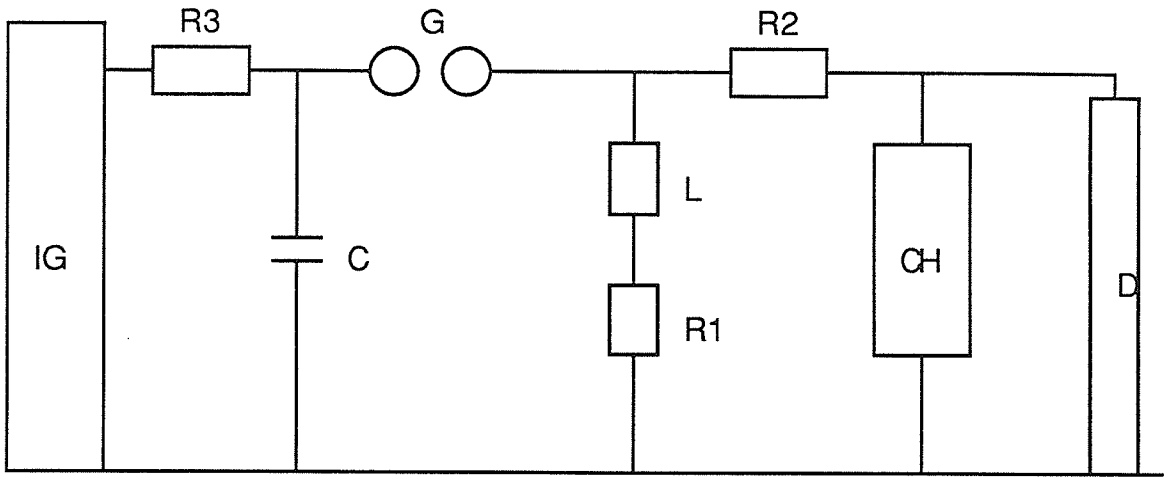


Figure 3.7: Bidirectional damped oscillatory impulse generating circuit.
IG-impulse generator; CH-test chamber; D-voltage divider;
R1,R2,R3-noninductive resistors; C-capacitor;L-inductance; G-sphere gap
R2= 206 Ω; R3= 35 kΩ

The typical waveforms of the bidirectional damped oscillatory impulse voltages with different frequency and damping factor are shown in Figure 3.8 -3.11, waveform parameters of the impulse voltage are shown in table 1. The damping factor is defined as the ratio of two subsequent amplitudes of the same polarity. The oscillation frequencies and the damping factors are determined from the oscillogram.

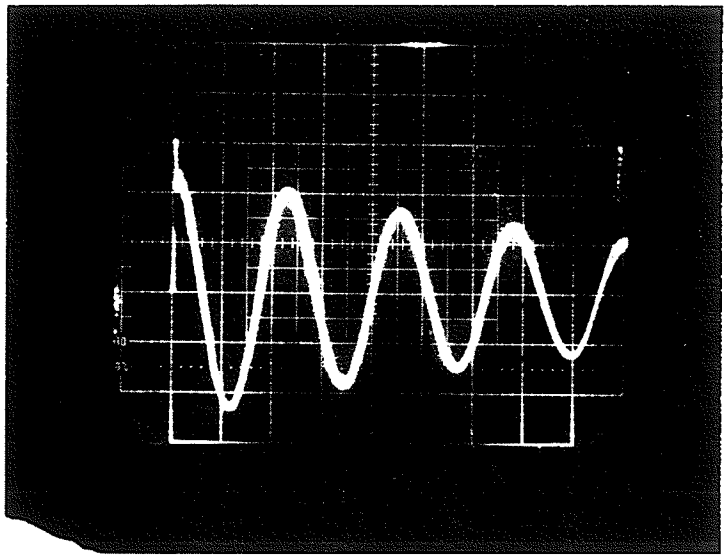

Figure 3.8: Bidirectional damped oscillatory impulse wavefront oscillogram.
Time: 2 μs/cm; Volt: 10 V/cm; f=0.2 MHz & δ=0.8

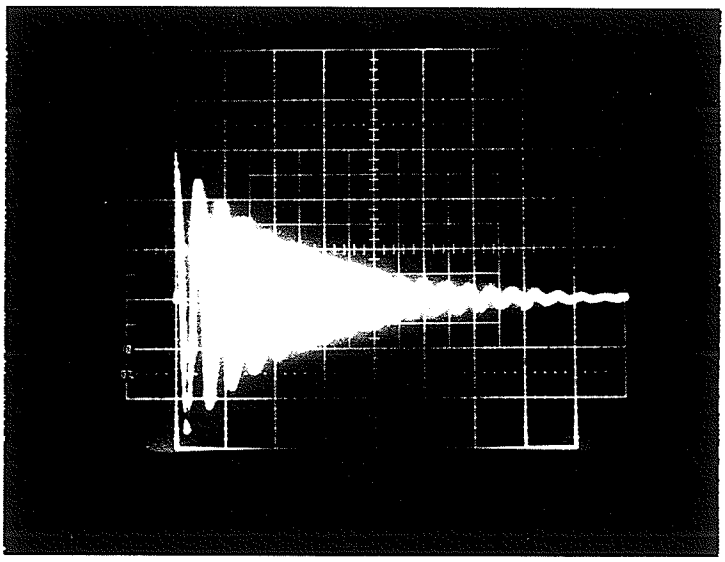

Figure 3.9: Bidirectional damped oscillatory impulse wavefront oscillogram.
Time: 10 μs/cm; Volt: 10 V/cm; f=0.2 MHz & δ=0.8

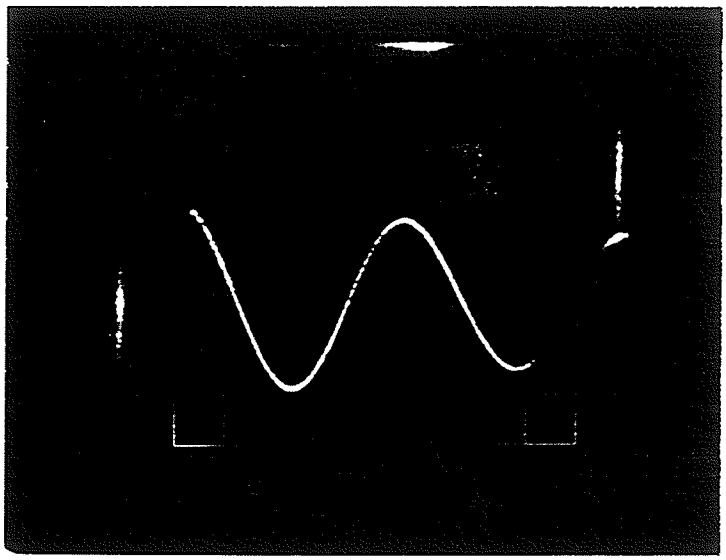

Figure 3.10: Bidirectional damped oscillatory impulse wavefront oscillogram.
Time: 0.2 μs/cm; Volt: 10 V/cm; f=1.15 MHz & δ=0.8

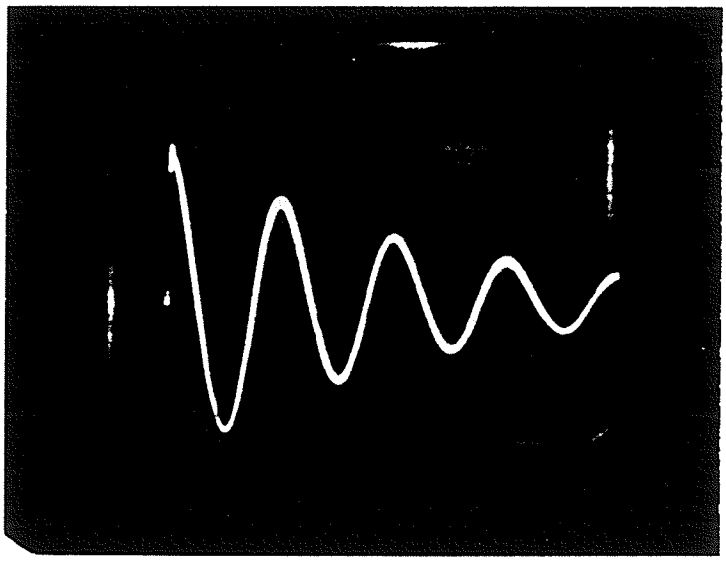

Figure 3.11: Bidirectional damped oscillatory impulse wavefront oscillogram.
Time: 2 μs/cm; Volt: 10 V/cm; f=0.2 MHz & δ=0.65

Table 1. Waveform parameters of bidirectional damped oscillatory voltages

(C, L and R1 are parameters of the circuit in Figure 3.7)

| Capacitance C | Inductance L | Series resistance R1 | Frequency f | Damping factor δ |
|---|---|---|---|---|
| 5000 pF | 100 μH | 0 | 0.2 MHz | 0.8 |
| 500 pF | 40 μH | 13 Ω | 1.15 MHz | 0.8 |
| 5000 pF | 40 μH | 0 | 0.35 MHz | 0.9 |
| 500 pF | 100 μH | 28 Ω | 0.7 MHz | 0.75 |
| 5000 pF | 70 μH | 13 Ω | 0.25 MHz | 0.65 |

### 3.3.2 Unidirectional oscillatory impulse circuit

The circuit to generate the unidirectional damped oscillatory impulse voltage is shown in Figure 3.12. Different oscillation frequency and damping factor can be obtained by adjusting inductance L and resistance R. The voltage v(t) across the test chamber is given by [22]

$$v(t) = A\,E\{e^{-\gamma t} - B\,e^{-\alpha t}\sin(\beta t+\theta)\} \qquad (3.2)$$

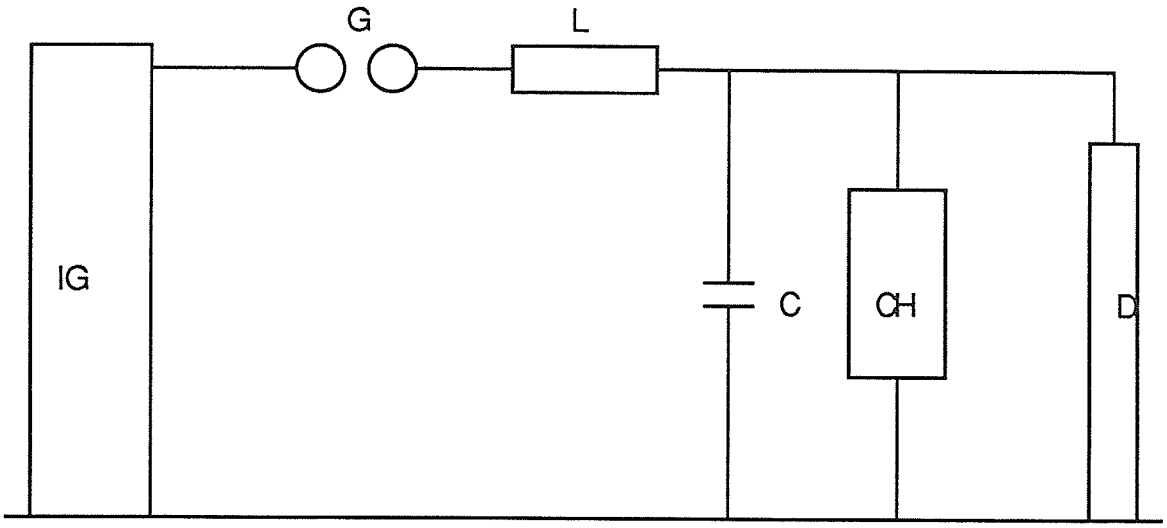


Figure 3.12: Unidirectional damped oscillatory impulse generating circuit.
IG-impulse generator; CH-test chamber; D-voltage divider;
C-capacitor;L-inductance; G-sphere gap
C= 5000 pF; L= 20 mH

Where E is the charging voltage of C and A, B, $\alpha$, $\beta$, $\gamma$, and $\theta$ are constants dependent on circuit parameter.

a typical waveform of an unidirectional damped oscillatory impulse voltage is shown in Figure 3.13, the damping factor is represented by the ratio of first peak amplitude V1 and second peak amplitude V2 or $\delta$ =V2/V1. The oscillation frequency and the damping factor are measured from the oscillogram.

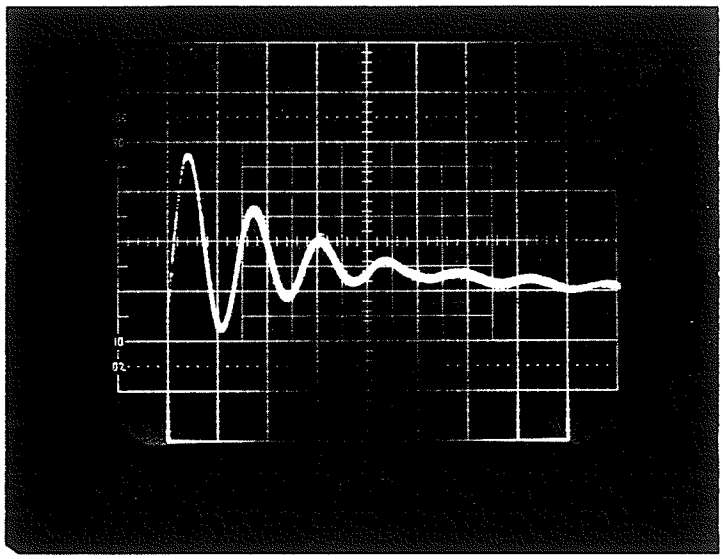

Figure 3.13: Unidirectional damped oscillatory impulse wavefront oscillogram.
Time: 50 μs/cm; Volt: 10 V/cm: f=15.5 kHz & δ=0.7

## 3.4 Experimental techniques

The experimental techniques used in this investigation under lightning, steep front and high frequency oscillatory impulse voltages are basically the same.

### 3.4.1 Test procedure

Impulse voltages were applied to the gaps and increased in steps starting from a suitable value until breakdown of the test gap occurred. Each increment in voltage was not more than 3% of the magnitude employed in the previous step. The wait interval between two impulse applications, when breakdown did not occur, was

3 minutes.

In this investigation, all tests were conducted with pressure in the test chamber at atmospheric. After each breakdown the test gap was examined to ascertain the location of breakdown. Breakdown on the surface caused surface damage which required prolonged application of vacuum for removal of bubbles. Following surface damage a new gap was used for subsequent testing. A similar procedure was followed when breakdowns occurred away from the interface; in this case a short time sufficed for removal of all bubbles by application of vacuum and the same gap was used for another test . In this manner, at least 5 tests could be conducted on each samples. In all cases the breakdown voltage , the breakdown time and the location of breakdown was noted. For each gap at least ten readings of breakdown voltage were obtained and the mean breakdown voltage, the mean breakdown time and the standard deviation computed.

### 3.4.2 Volt-time characteristics measurements

The method for the measurement of volt-time characteristics under a standard impulse waveshape (1.47/47 μs) is illustrated in Figure 3.14. A similar procedure was used in the case of steep front impulse (0.15/15 μs) and oscillatory impulses . The first step of this procedure was to determine the 50 % surface breakdown voltage ( indicated by an arrow in the figure), which was determined by using the " up and down " method. Next the 50 % breakdown voltage was used as the first voltage level for the voltage-time characteristics measurements and then the applied voltage level was increased while keeping the voltage waveshape the same until the second desired voltage value was obtained. Using the same manner, the volt-time curve was determined. It need to note that when chopping was on the tail of the impulses , the breakdown voltages recorded was the peak value of the impulse

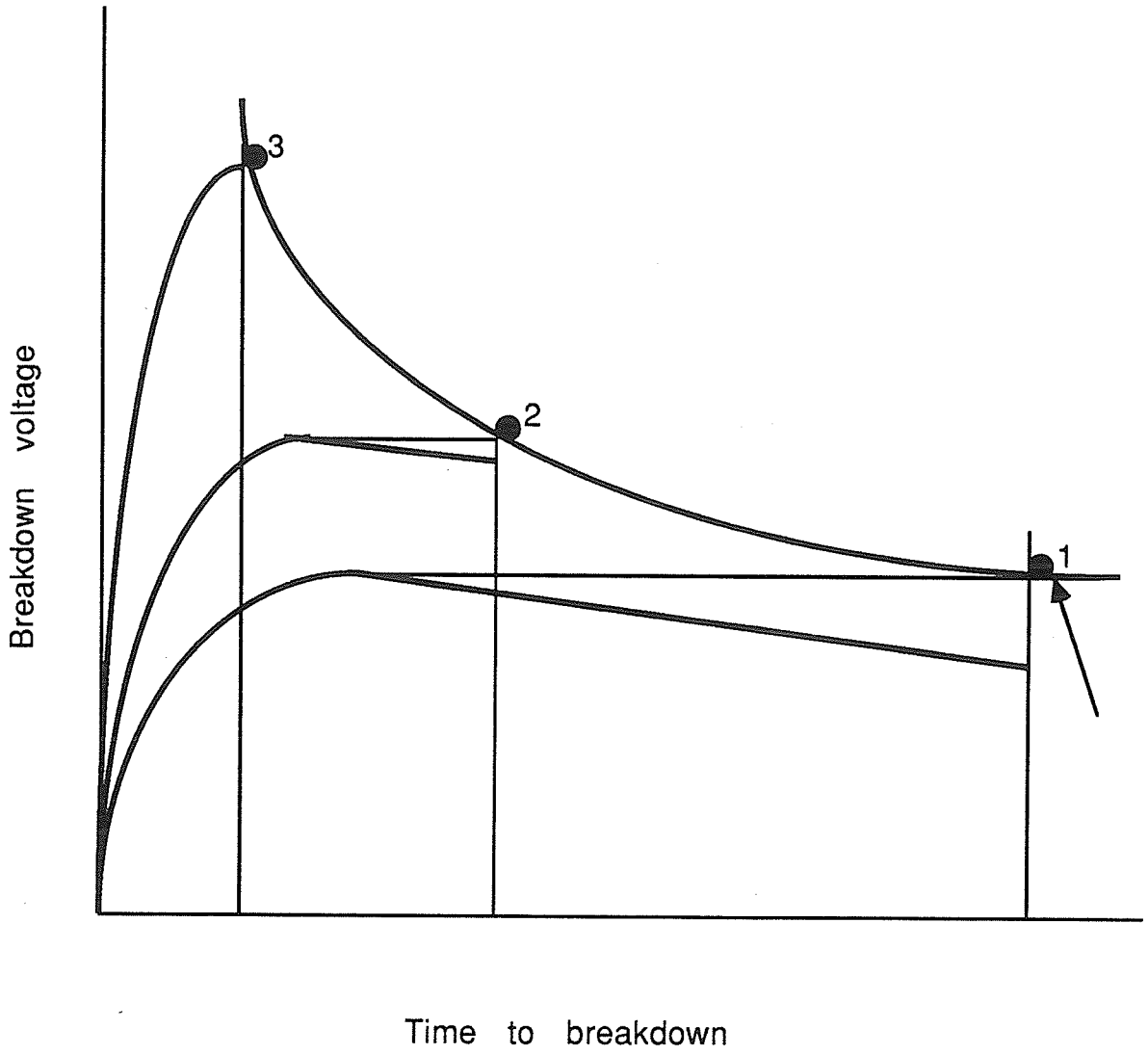


Figure 3.14: Method for determination volt-time characteristics

voltage; while chopping was on the front of the impulses , the breakdown voltage recorded was the actual breakdown voltage of the impulses. For each voltage level, at least 10 voltage applications were made and the breakdown voltages and times to breakdown were recorded after each breakdown. The breakdown times were determined according to the IEEE standard [29] from the virtual origin to the instant that the applied voltage collapsed. In all cases, the interval between successive breakdown was at least 30 minutes to allow complete recovery of the gap.

# CHAPTER 4

# EXPERIMENTAL RESULTS AND DISCUSSION

## 4.1 Volt-time Characteristics of Processed Pressboard Under Lightning Impulse Voltage

Since the electrode arrangement of a solid-liquid interface parallel to the electrical field is often found in practical apparatus, it is necessary to know the surface breakdown behavior of the processed pressboard from the point of view of insulation coordination.

Figure 4.1 shows the experimentally determined surface strength volt-time characteristics of processed pressboard in mineral oil. The characteristics were found by application of standard lightning impulse voltages to a gap length of 10 mm at room temperature and each point in this curve and also in all the succeeding volt-time curves in this chapter represent the average value of at least 10 breakdown voltages. As can be seen from the figure the breakdown values decrease with increase in the breakdown time and the curve gradually flattens out. With increasing overvoltage, it was found that the breakdown values are less scattered and also more damage was caused on the surface of pressboard.

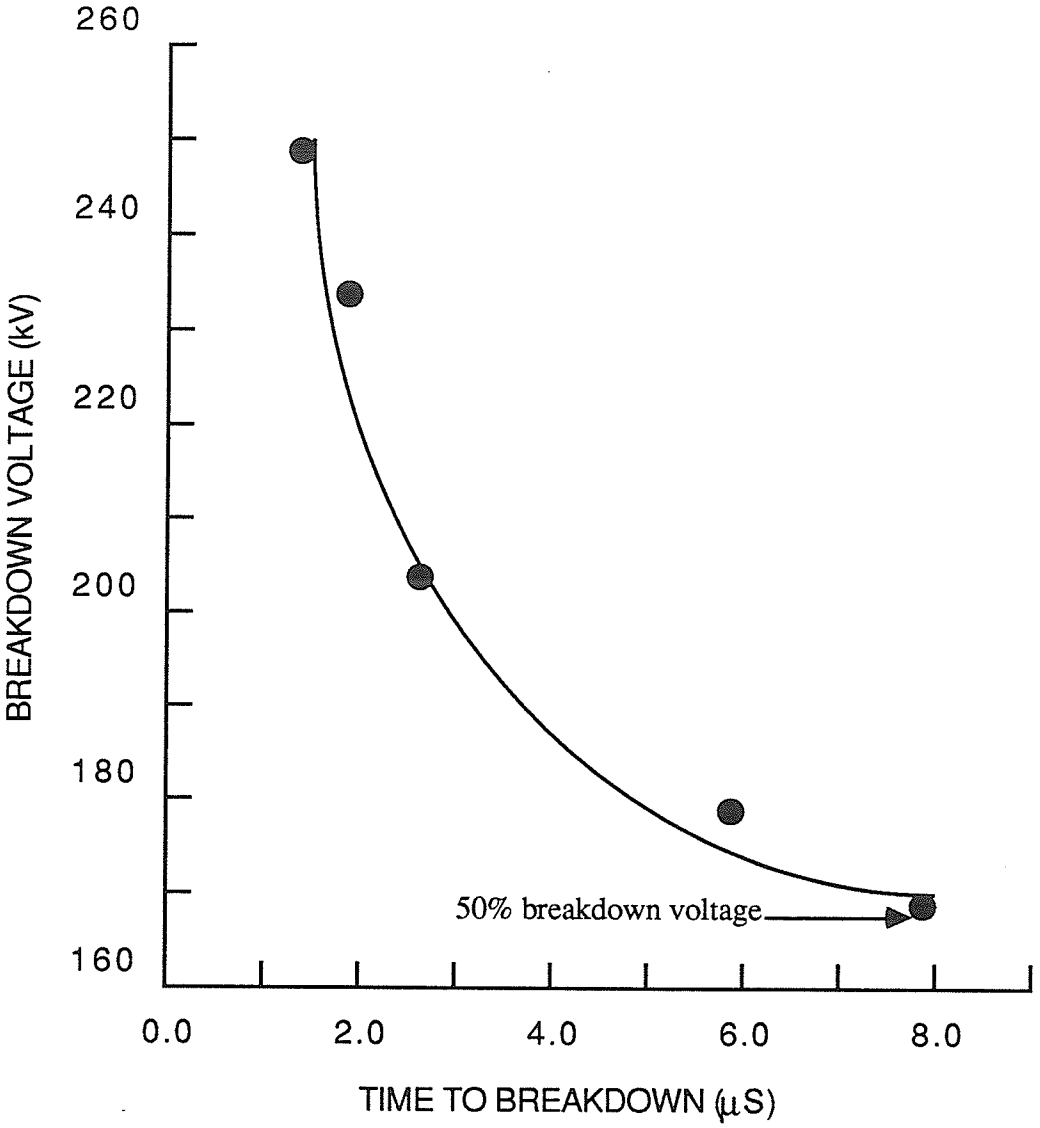


Figure 4.1: Surface strength Volt-time characteristics of mineral oil processed pressboard under lightning impulse : 10 mm gap

It is interesting to note that , in this case, the 50% surface breakdown voltage , which was indicated by an arrow in the figure, approximately equal to the 50 % breakdown value reported in [8].

## 4.2 Volt-time Characteristics of processed pressboard under steep front impulse voltage

Although extensive researches have been done on the behaviors of the dielectric strength behaviors of SF6 gas insulation under steep front impulses , there are scant published data available on the surface strength of oil-impregnated paper insulation under fast rising impulses. In the studies involving SF6 gas , an abnormal phenomenon was observed under fast rising voltage [28, 30-32]; these authors found that the breakdown voltage did not always increase as the breakdown time become shorter . The breakdown voltage obtained under steep front impulses was less than that obtained under standard lightning impulse voltages for the same time to breakdown. This phenomenon is very important because the electrical power system may at times be subjected to fast rising voltages. In this section the volt-time characteristics of oil-impregnated paper under steep front impulse has been reported. Furthermore comparison of the characteristics under standard lightning impulse (section 4.1) and steep front impulse enables one to ascertain whether oil-impregnated paper insulation exhibit a similar behavior as SF6 gas insulation.

Figures 4.2 and 4.3 show the surface strength volt-time characteristics of processed pressboard under steep front impulse voltages for gap lengths of 5

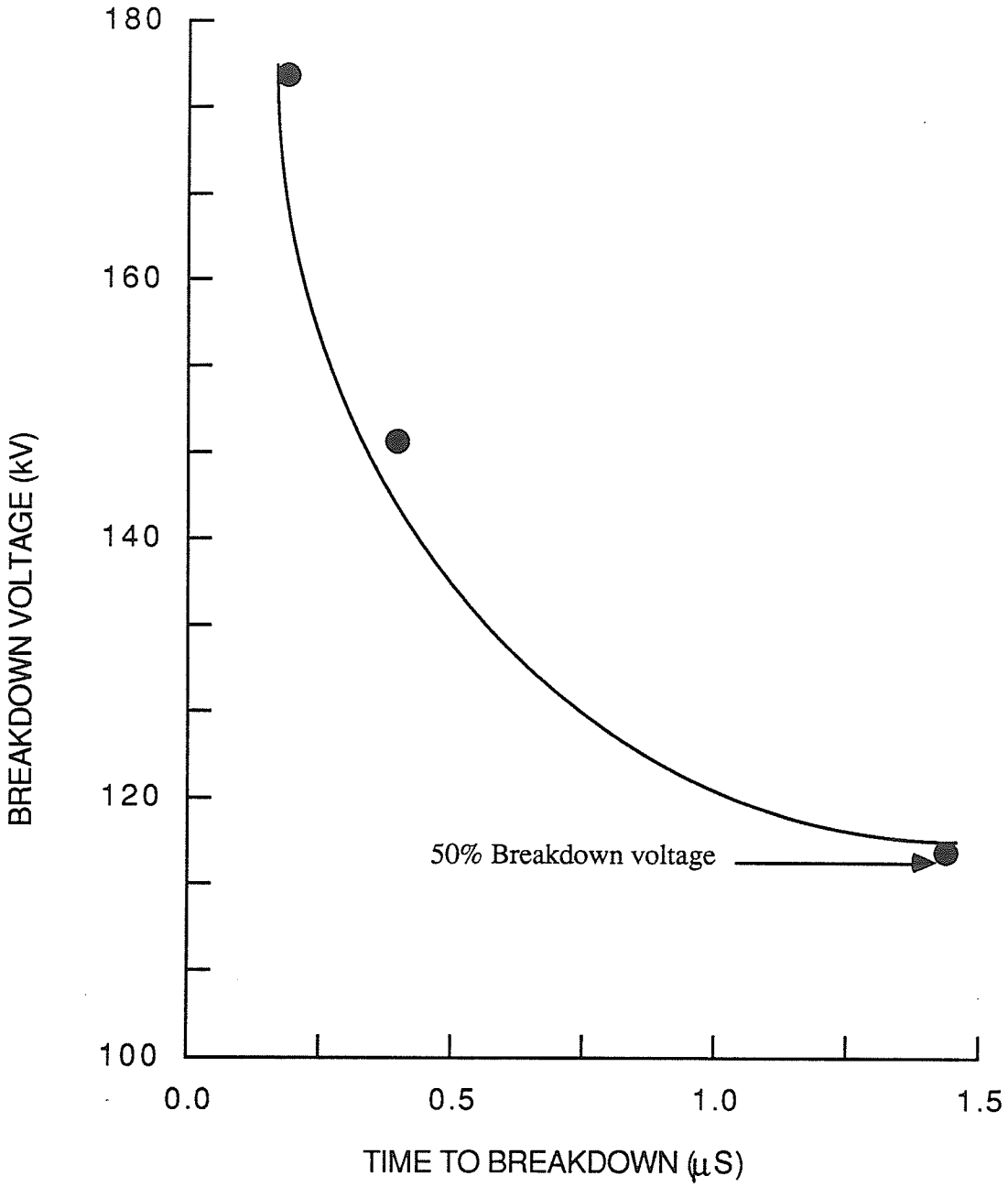


Figure 4.2: Surface strength Voltage-time characteristics of mineral oil processed pressboard under steep front impulse : 5 mm gap

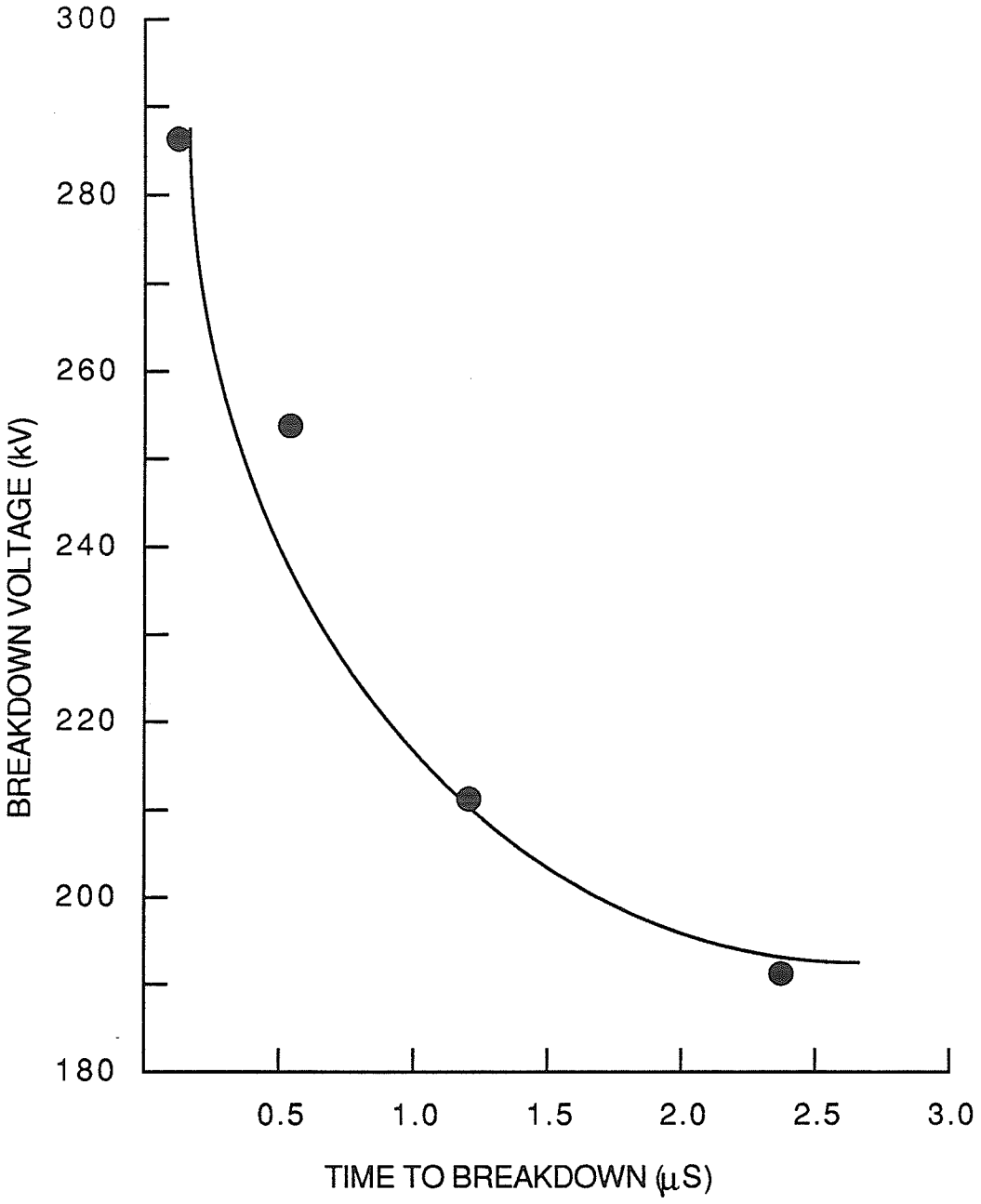


Figure 4.3: Surface strength Voltage-time characteristics of mineral oil processed pressboard under steep front impulse : 10 mm gap

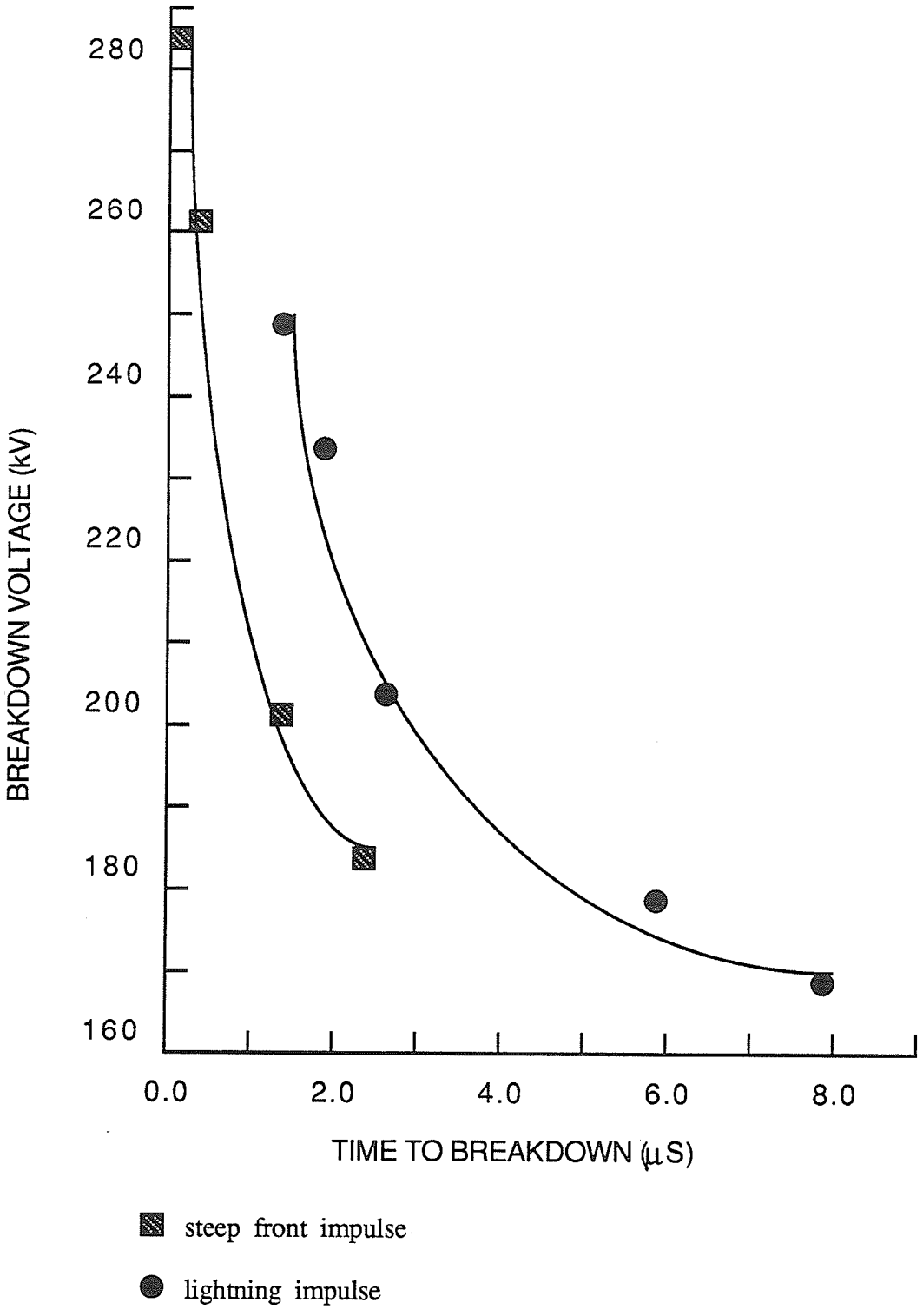


Figure 4.4: Surface strength Voltage-time characteristics of mineral oil processed pressboard under steep front impulse and lightning impulse : 10 mm gap

mm and 10 mm respectively. As can be seen from Figure 4.2, for the 5 mm gap the surface breakdown voltages decrease sharply with increase in breakdown time to about 1.0 μs after which the breakdown voltage is insensitive to breakdown time. For the 10 mm gap , the volt-time characteristics follow a similar trend. The volt-time curves for the 10 mm gap under both steep front and lightning impulses are presented in Figure 4.4. Although the curves follow a similar trend, the slope of the curve under steep front impulses is generally steeper than that under lightning impulses. An abnormal phenomenon which was reported in [28, 30] was also observed in this study. As can be seen from Figure 4.4 the characteristics obtained under steep front impulses are significantly lower than those obtained under lightning impulses in the time interval from 1.5 to 2.7 μs. This phenomenon is particularly important for the insulation coordination of electrical power systems.

It was observed that the surface breakdown values are less scattered but cause more surface breakdowns under steep front impulses than under lightning impulses for the 10 mm gap. A typical chopped steep front waveshape impulse voltage is shown in Figure 4.5.

## 4.3 Volt-time Characteristics of Processed Pressboard under Oscillatory Impulse Voltages

Although oscillatory impulse voltages are one of the main types of non-standard impulses that have gained widespread acceptance in test standards [24], information on the breakdown characteristics of oil paper insulations under these voltages is rather scanty, particularly in the high

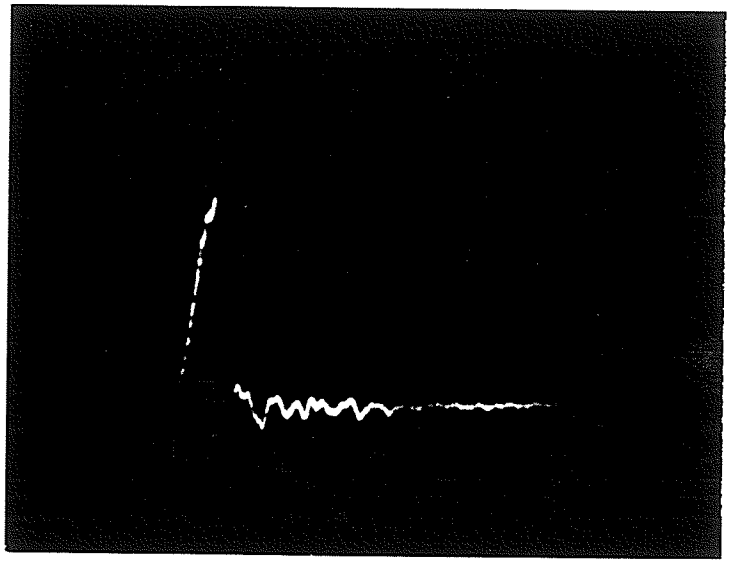

Figure 4.5: Chopped steep front impulse wavefront oscillogram: positive polarity. Time: 0.2 μs/cm; Volt: 5 V/cm

frequency range, i.e. several hundred kilo-Hertz [ 20, 22]. Hence, the main intent of this investigation was to obtain surface breakdown experimental data of processed pressboard under high frequency oscillatory impulses.

### 4.3.1 Surface breakdown characteristics under oscillatory impulse with frequency f=0.2 MHz and damping factor δ=0.8

Figure 4.6 shows the surface strength volt-time characteristics of the processed pressboard under cos-bidirectional impulse voltages with frequency f = 0.2 MHz and damping factor $\delta = 0.8$. As can be seen from Figure 4.6, the surface breakdown voltage decreases continuously with increase in breakdown time and the slope is generally less steep than that obtained under steep front impulse. A comparison of the surface strength volt-time curves of processed pressboard under

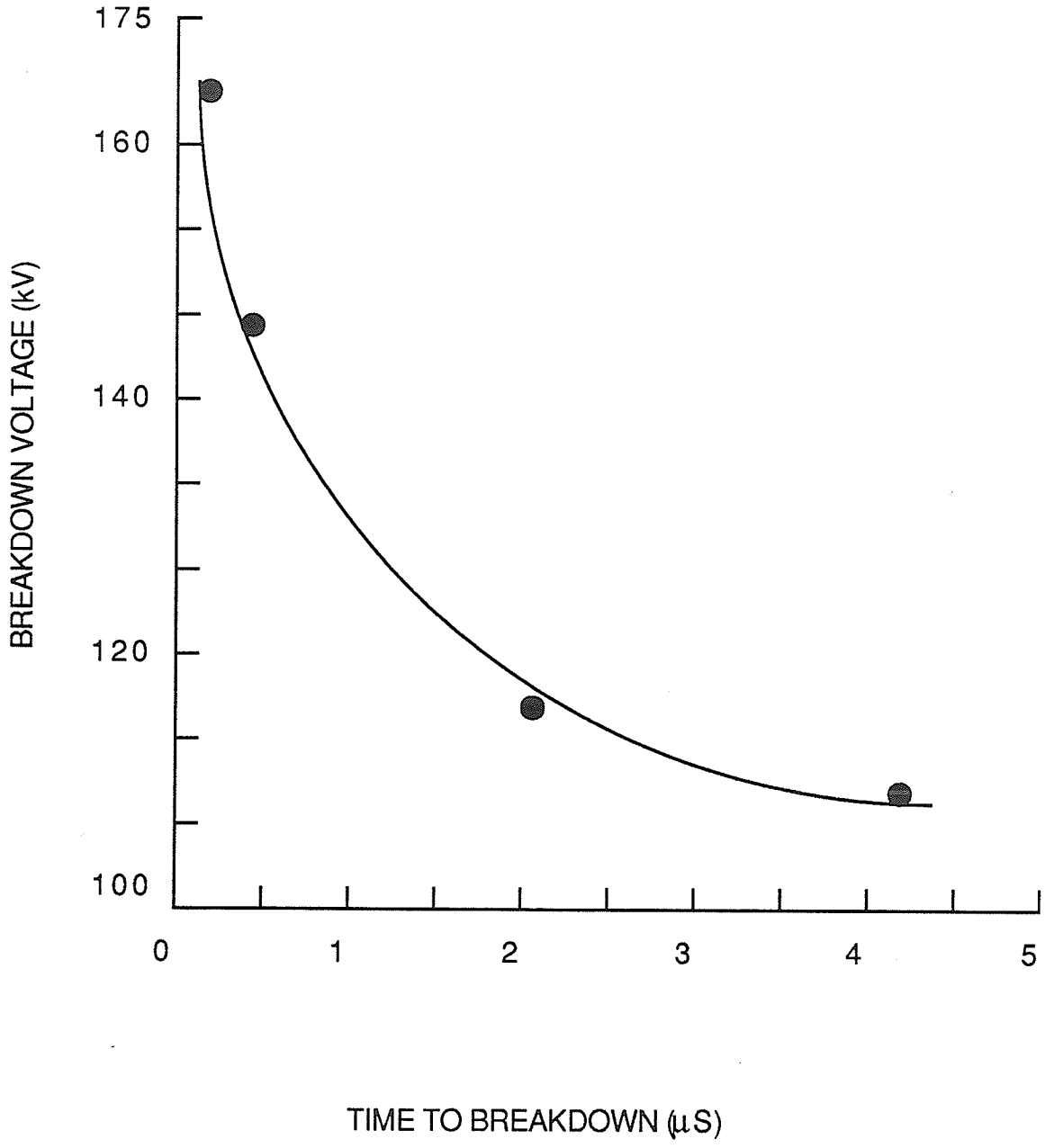


Figure 4.6: Surface strength Voltage-time characteristics of mineral oil processed pressboard under oscillatory cos-bidirectional impulse with frequency f=0.2 MHz, damping factor $\delta$=0.8 : 5 mm gap

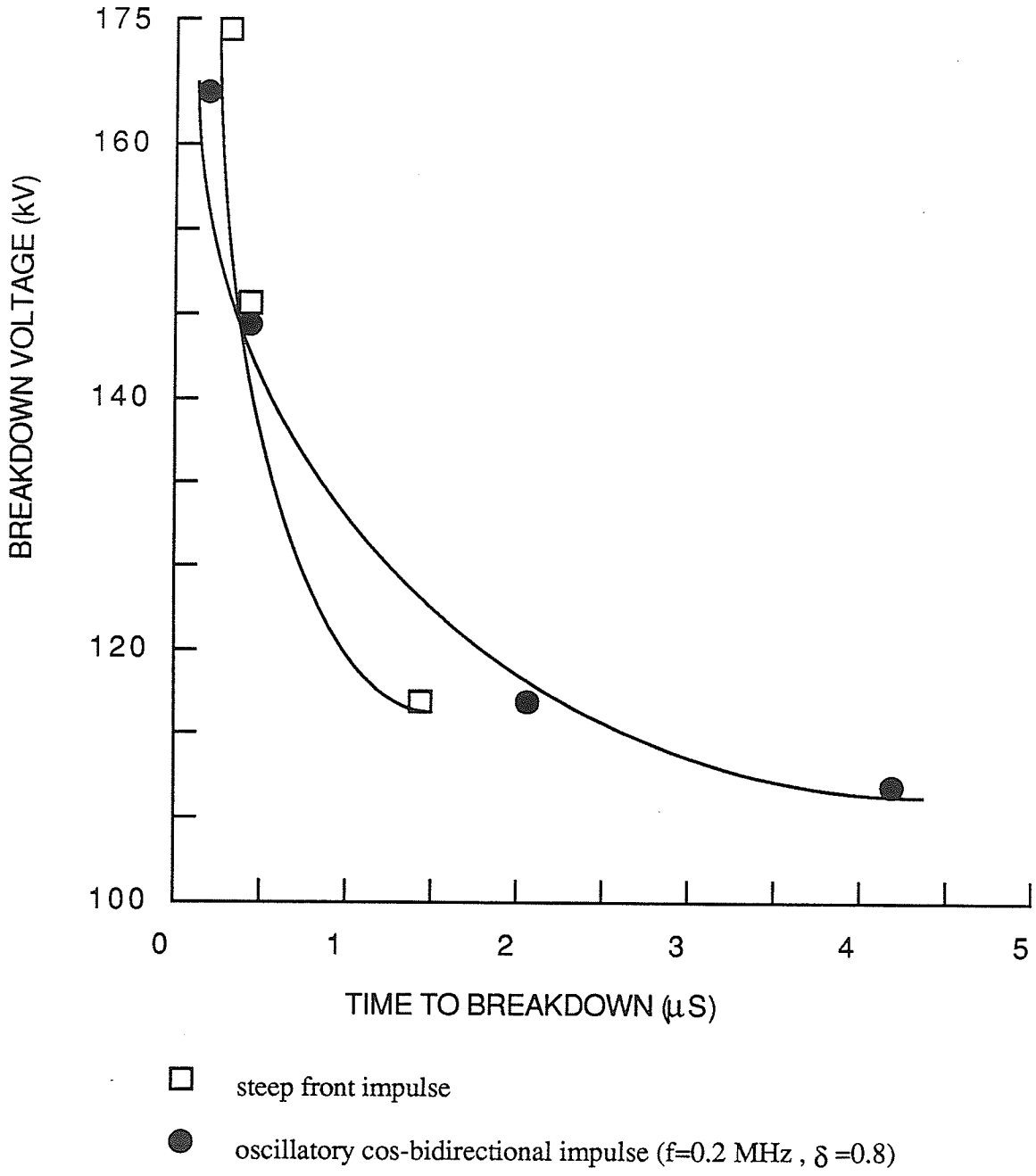


Figure 4.7: Surface strength Voltage-time characteristics of processed pressboard under oscillatory cos-bidirectional ( f=0.2 MHz, δ=0.8 ) and steep front impulse : 5 mm gap

both steep front and oscillatory cos-bidirectional impulse voltages is shown in Figure 4.7. It was found that the breakdown did not always occur on the first voltage crest but sometimes as late as on the fourth peak.An anomalous behavior was also observed; the surface breakdown voltage of processed pressboard under oscillatory voltage is lower than that under steep front impulse voltage in the time range of 0.15 - 0.65 μs but becomes higher than that with further increase in breakdown time. The reason for this behavior is explained in Chapter 5 . A typical chopped waveshape of the oscillatory impulse voltage (f=0.2 MHz; δ=0.8) is shown in Figure 4.8.

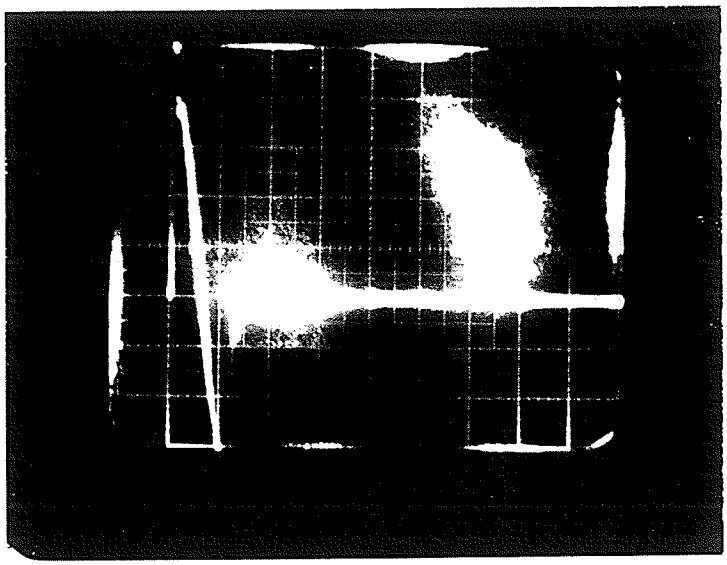

Figure 4.8: Chopped oscillatory impulse wavefront oscillogram:
f=0.2 MHz, δ=0.8; Time: 0.2 μs/cm; Volt: 20 V/cm

### 4.3.2 Surface breakdown characteristics under oscillatory impulse with frequency f=1.15 MHz and damping factor $\delta$=0.8

The surface strength volt-time characteristics of processed pressboard under oscillatory cos-bidirectional impulse voltage with frequency f = 1.15 MHz and damping factor $\delta$ = 0.8 is shown in Figure 4.9. In this case, the surface breakdown voltages decrease sharply with the increase of breakdown time. Figure 4.10 shows the comparison of volt - time characteristics under the oscillatory impulse voltages with frequency f = 0.2 MHz and f = 1.15 MHz at the same damping factor $\delta$ = 0.8. Although the curves follow a similar trend, the slope of the characteristics under frequency f = 1.15 MHz is steeper than that under f = 0.2 MHz. As can be seen from the Figure 4.10, the surface breakdown strength under oscillatory impulse with a higher frequency ( f = 1.15 MHz ) is generally lower than that under impulse with a lower frequency ( f = 0.2 MHz ) . However an interesting behavior was noted in the time range 0.2 - 0.6 $\mu$s ; the surface strength under oscillatory impulse with frequency f = 1.15 MHz becomes almost the same as that with frequency f = 0.2 MHz; after 0.6 $\mu$s the difference in the breakdown voltage becomes larger as the breakdown time increases .

It is seen in Figure 4.10 that the 50 % breakdown value for frequency f = 0.2 MHz is only slightly higher that that for f = 1.15 MHz. This indicates that the effect of frequency on the 50 % surface breakdown voltages is small.

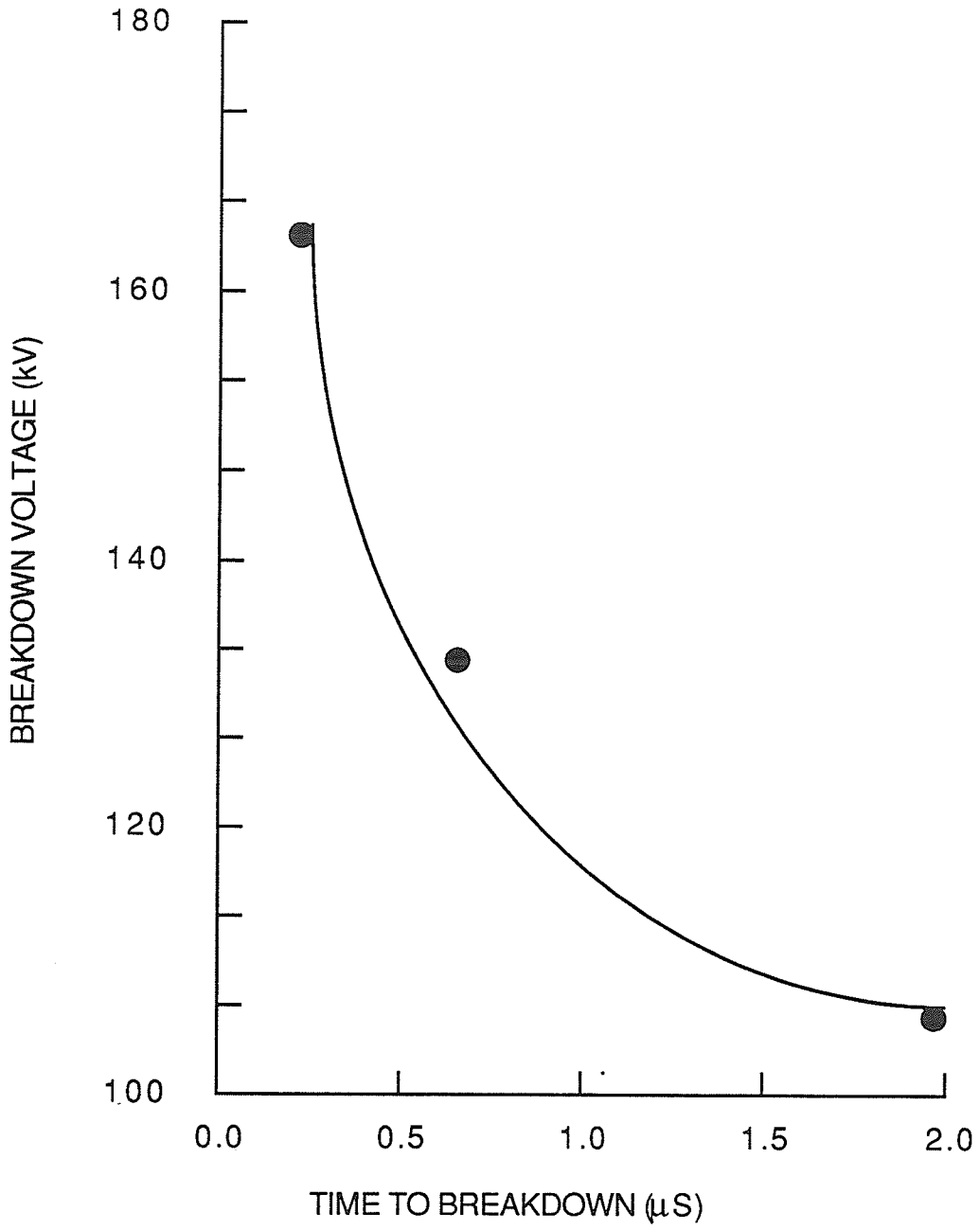


Figure 4.9: Surface strength Voltage-time characteristics of processed pressboard under oscillatory cos-bidirectional impulse with frequency f=1.15 MHz and damping factor $\delta$=0.8 : 5 mm gap

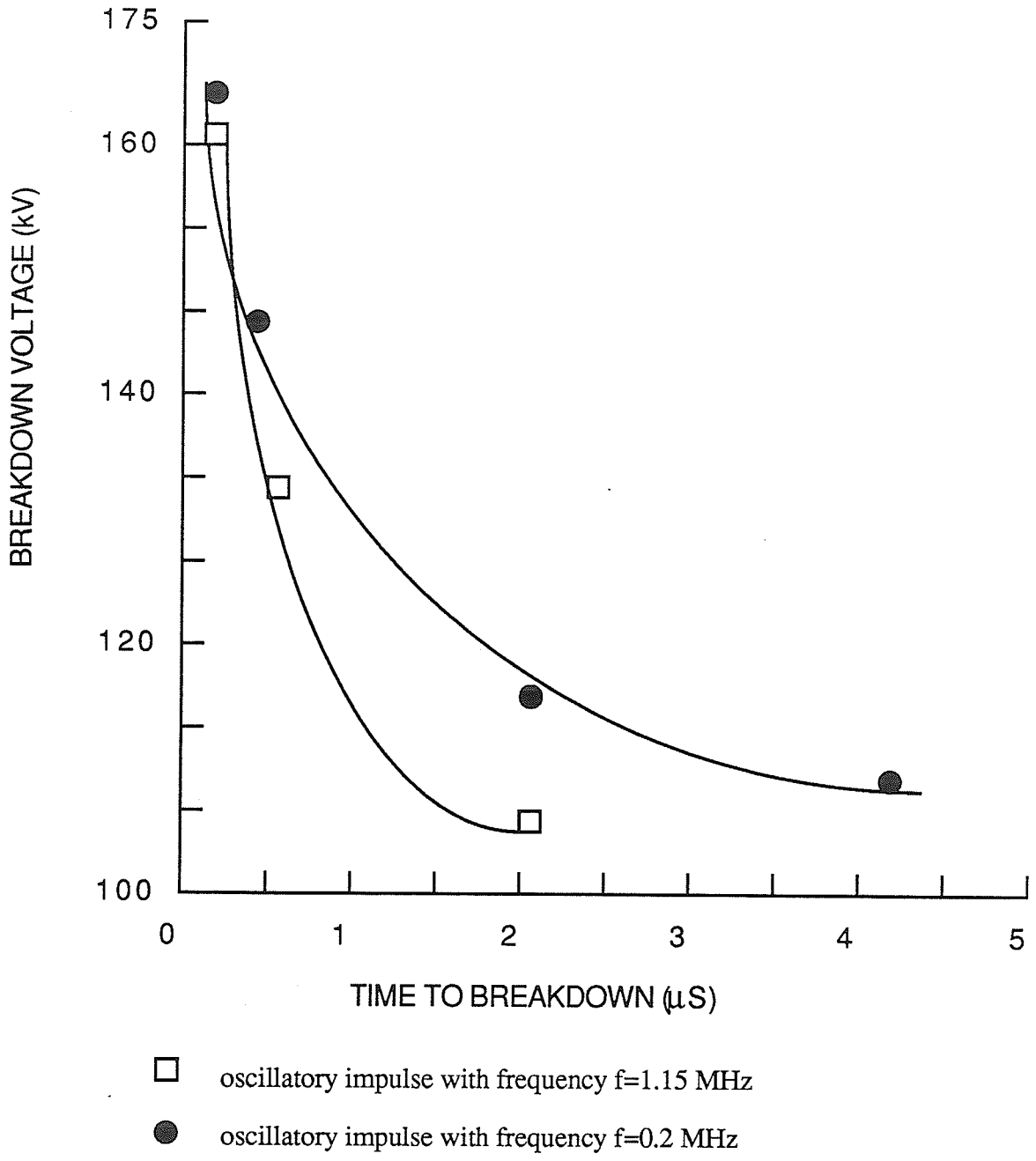


Figure 4.10: Surface strength Voltage-time characteristics of processed pressboard under oscillatory cos-bidirectional impulse with frequency f = 1.15 MHz and f = 0.2 MHz at the same damping factor $\delta = 0.8$: 5 mm gap

### 4.3.3 Surface breakdown characteristics under oscillatory impulse with frequency f=0.2 MHz and damping factor δ=0.65

The surface strength volt-time characteristics of processed pressboard under oscillatory cos-bidirectional impulse voltage with frequency f = 0.2 MHz and damping factor $\delta = 0.65$ is shown in Figure 4.11. In this case, the 50% surface breakdown voltage is higher than that obtained under steep front impulse and oscillatory impulse with a higher damping factor (Figure 4.7). Figure 4.12 shows a comparison of volt-time characteristics under the oscillatory impulse voltages with $\delta = 0.8$ and $\delta = 0.65$ at a frequency f = 0.2 MHz. As can be seen from the figures, the two curves almost follow the same trend. the surface breakdown strength under oscillatory impulse with a lower damping factor ( $\delta = 0.65$ ) is generally higher than that under impulse with a higher damping factor ( $\delta = 0.8$ ).

With a lower damping factor ( $\delta = 0.65$ ) the surface breakdown always occurred on the first peak. No breakdown was ever recorded after the first peak. In general, the 50 % breakdown voltage increases with a decrease in the damping factor and the probability of a breakdown occurring after the first crest is decreased. With a lower damping factor ( $\delta = 0.65$ ), the breakdown depends only on the first voltage peak.

It is important to note that breakdown on the surface of processed pressboard under oscillatory impulse with a lower damping factor causes more serious damage than those under steep front impulse and oscillatory impulse with a higher damping factor.

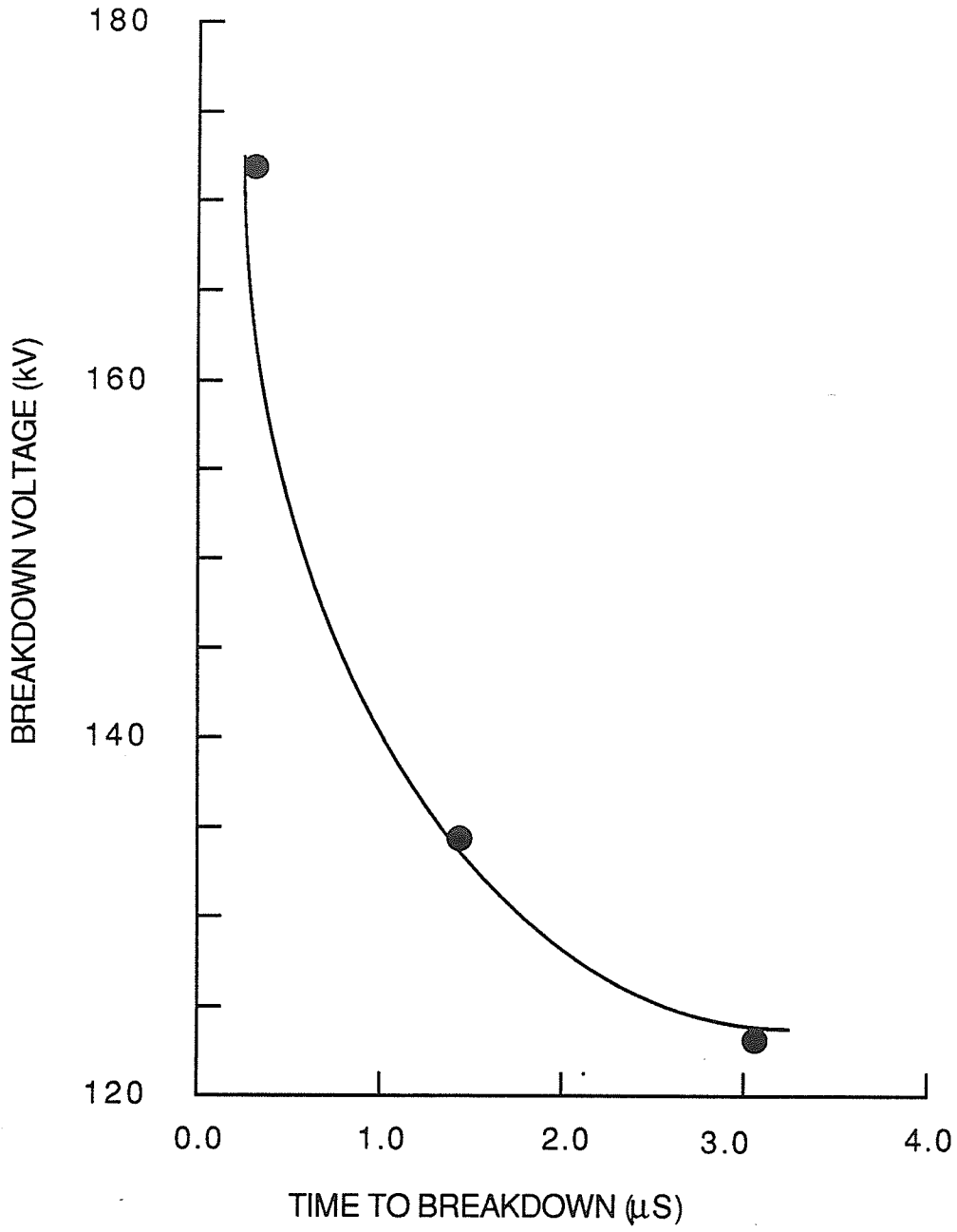


Figure 4.11: Surface strength Volt-time characteristics of processed pressboard under oscillatory cos-bidirectional impulse with frequency f=0.2 MHz and damping factor $\delta$=0.65: 5 mm gap

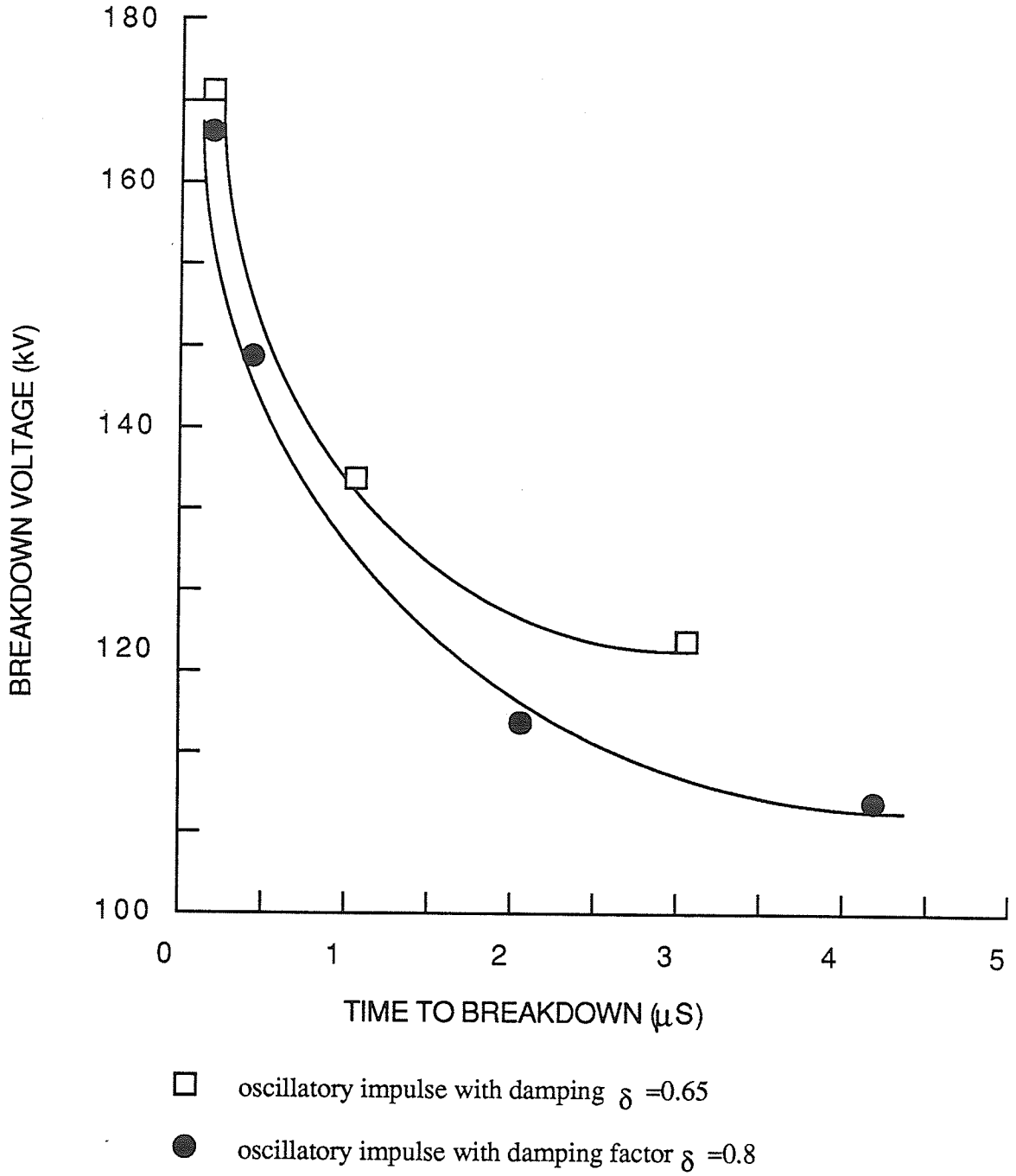


Figure 4.12: Surface strength Volt-time characteristics of processed pressboard under oscillatory cos-bidirectional impulse with frequency damping factor δ=0.65 and δ=0.8 at the same frequency (f=0.2 MHz): 5 mm gap

## 4.4 Voltage-time Characteristics of Processed pressboard in aged oil

In order to evaluate the surface breakdown behavior of processed pressboard completely, tests were also conducted for 5 mm gap under steep front impulses and oscillatory impulse ( $f = 0.2$ MHz and $\delta = 0.8$ ) using aged oil which was obtained from a transformer in service in the Manitoba Hydro system ; the oil has aged for 15 years ( its aged properties has been presented in chapter 2 and compared with the properties of the unaged oil ). The surface breakdown voltages of processed pressboard in the aged oil under steep front and oscillatory impulses are shown in Figure 4.13 and Figure 4.14. As can be seen from these figures, the surface breakdown strengths in the aged oil are much lower than those in the new oil. The 50 % breakdown strength decreased approximately by 25 % and 32 % under steep front and oscillatory impulses respectively. The comparison of the volt-time curves of processed pressboard in both new and aged oil under steep front and oscillatory impulses are shown in Figure 4.15 and Figure 4.16. In both cases, the curves again follow the same trend, i.e. breakdown voltage decreases continuously with increase in breakdown time, but the slope of the curve obtained with aged oil is generally steeper than that obtained with new oil.

It is interesting to note that no surface breakdowns were observed in the aged oil under both steep front or oscillatory impulses. The reason is probably because the strength of the aged oil is so weak that breakdowns always occurred in the oil.

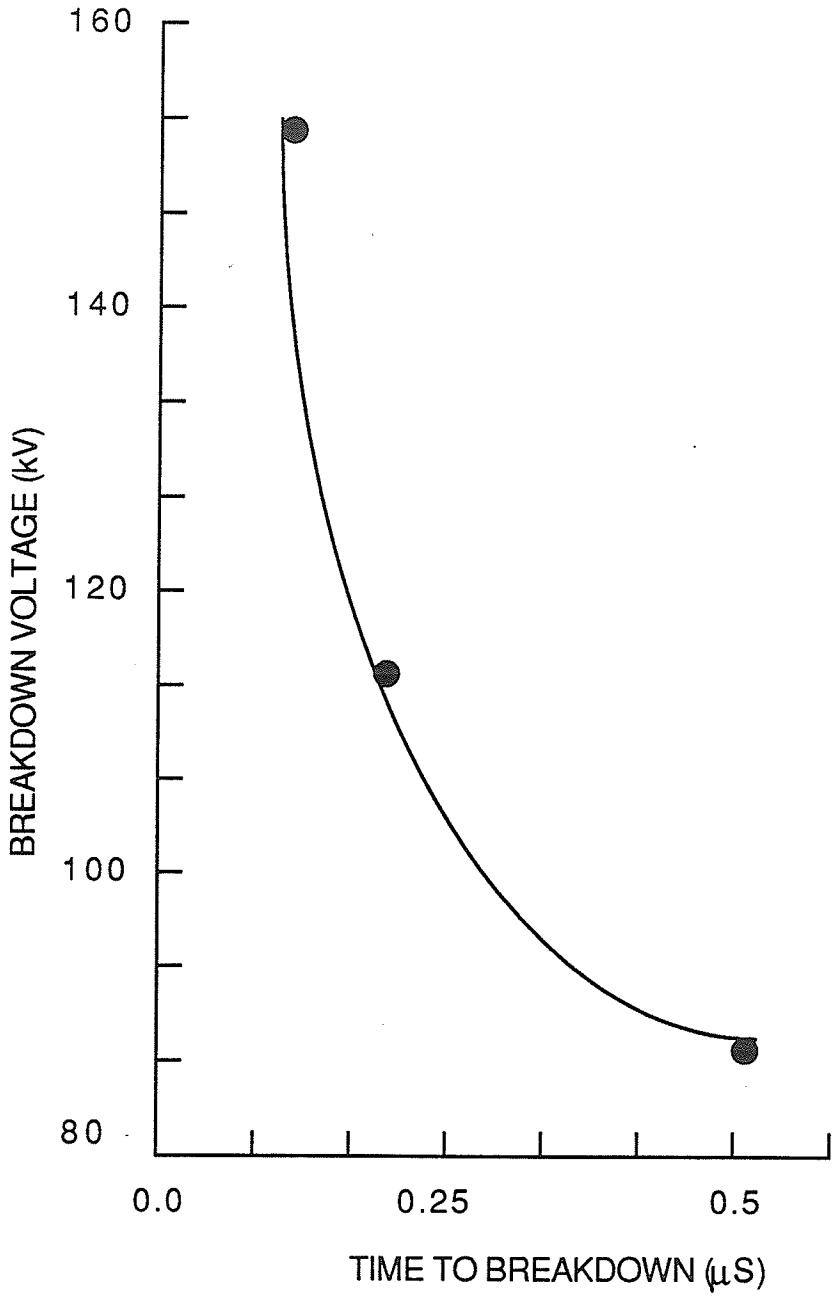


Figure 4.13: Surface strength Volt-time characteristics of processed pressboard in aged oil under steep front impulse: 5 mm gap

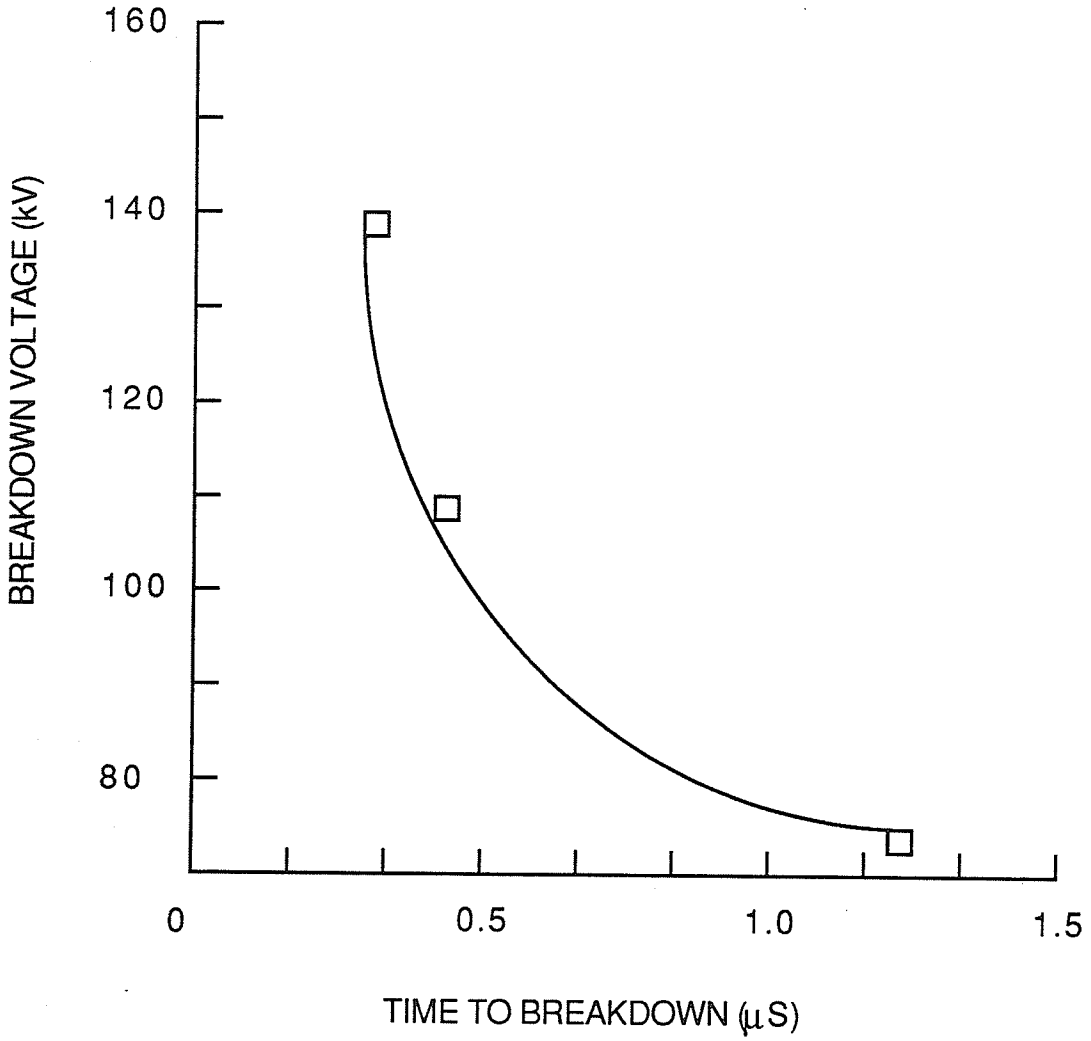


Figure 4.14: Surface strength Volt-time characteristics of processed pressboard in aged oil under oscillatory impulse : 5 mm gap

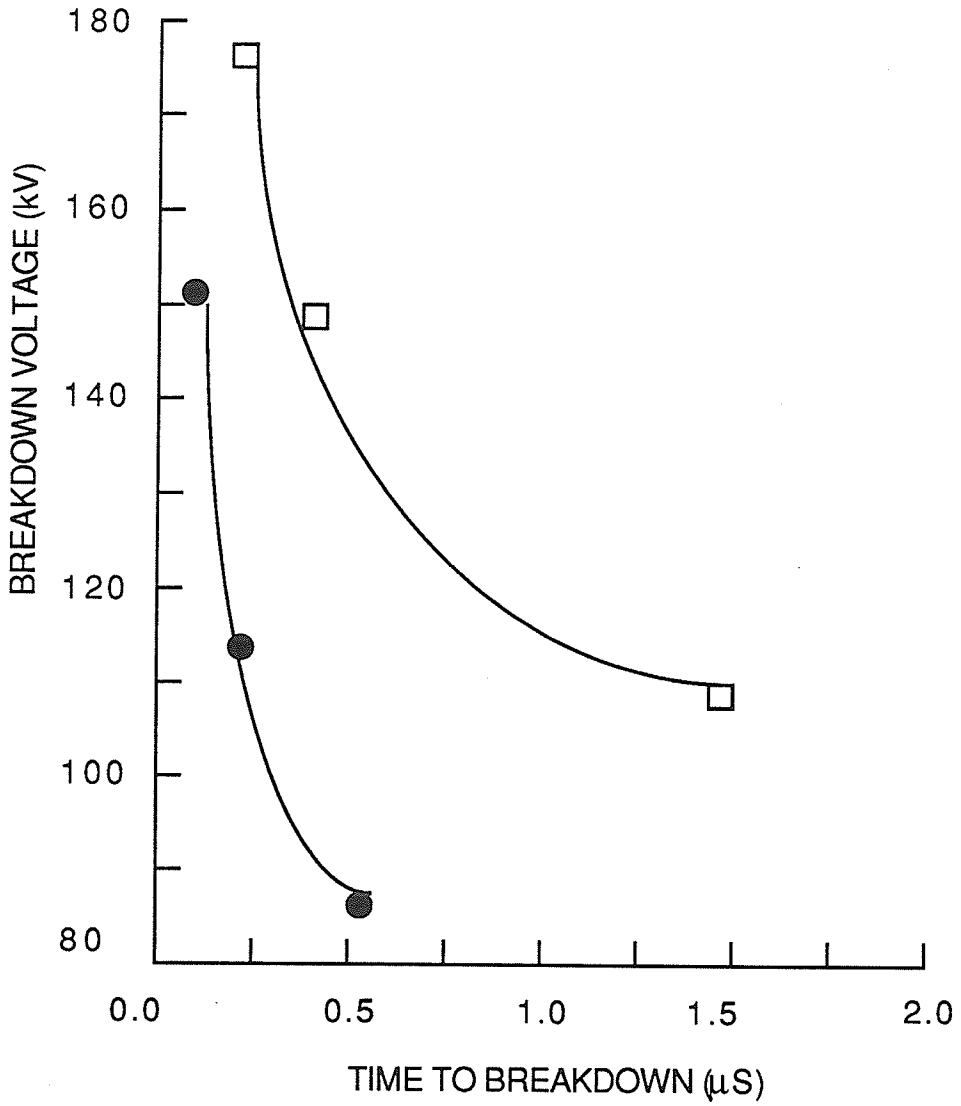


Figure 4.15: Surface strength Voltage-time characteristics of processed pressboard under steep front impulse in both new and aged oil : 5 mm gap

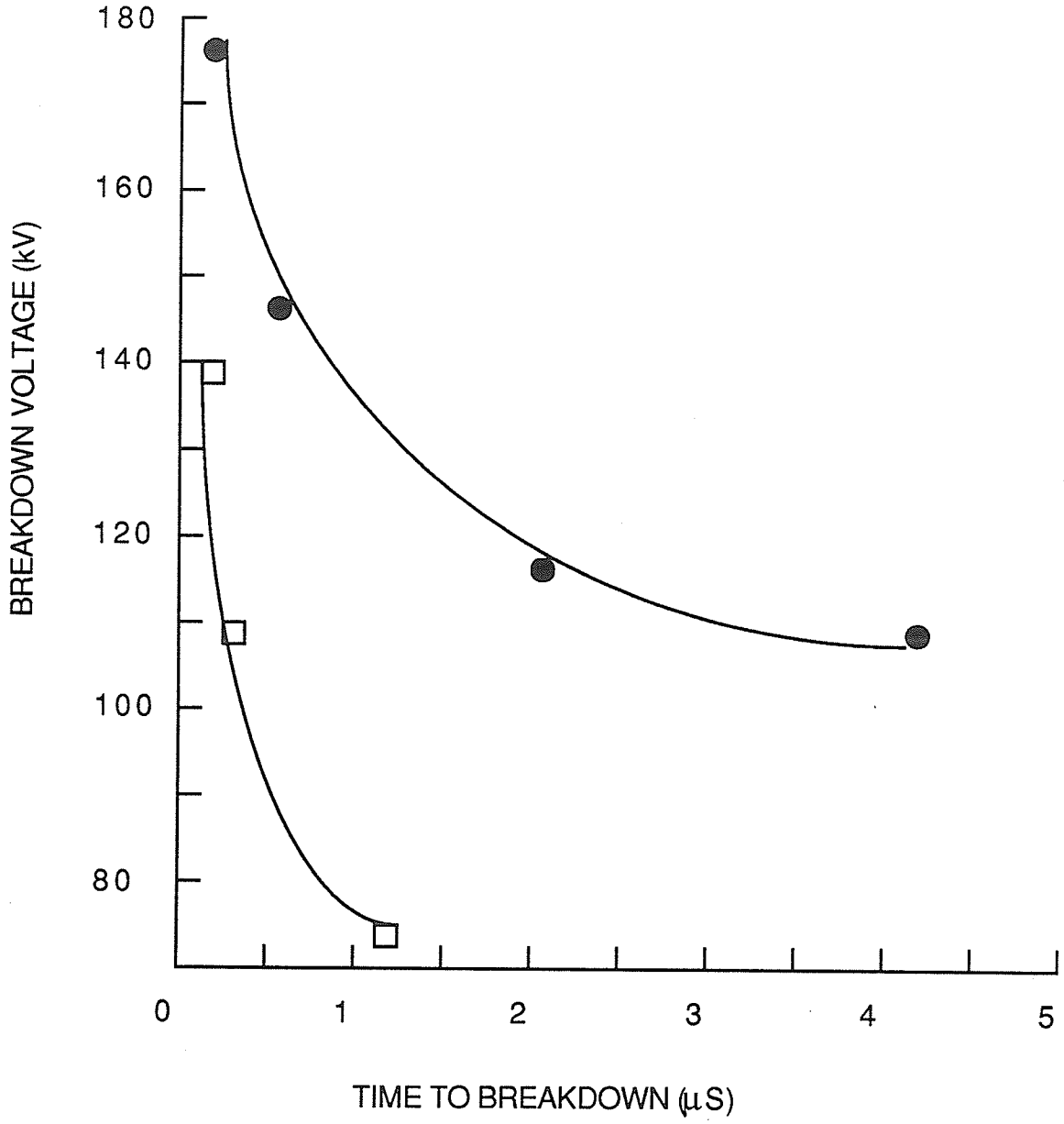


Figure 4.16: Surface strength Voltage-time characteristics of processed pressboard under oscillatory cos-bidirectional impulse ( f=0.2 MHz, $\delta$= 0.8 ) in new oil and aged oil : 5 mm gap

## 4.5 Discussions

Figure 4.17 shows a comparison of the surface breakdown voltages for the 5 mm gap under steep front and oscillatory impulses; the latter with different frequencies and damping factors. Although all the curves follow a similar trend, the slopes of the curves are totally different. This is particularly important from the point of view of insulation coordination. As can be seen from the figure, the differences in the breakdown voltages are small for breakdowns which take place in times 0.2 to 0.6 μs after which the differences increase sharply with increase of breakdown time. Reduction of the surface strength under steep front impulse were observed comparing with lightning impulse in the same time interval. This phenomena will be explained in the next Chapter.

It was found that the breakdown values are less scattered when breakdown occurred in the front than in the tail under both steep front impulse or oscillatory impulses.

The 50 % breakdown voltages under different impulses are tabulated in table 5.1. The lowest 50 % breakdown voltage with new oil is found under the application of standard lightning impulses. It is interesting to note that the 50 % breakdown values under oscillatory impulse voltages with frequency $f = 1.15$ MHz and $f = 0.2$ MHz and with the same damping factor ( $\delta = 0.8$ ) are respectively only 3 % and 8 % higher than those under lightning impulses . This means that the electrical strength under the oscillatory impulses with a damping factor of 0.8 is almost the same as that under the standard lightning impulses and the frequency

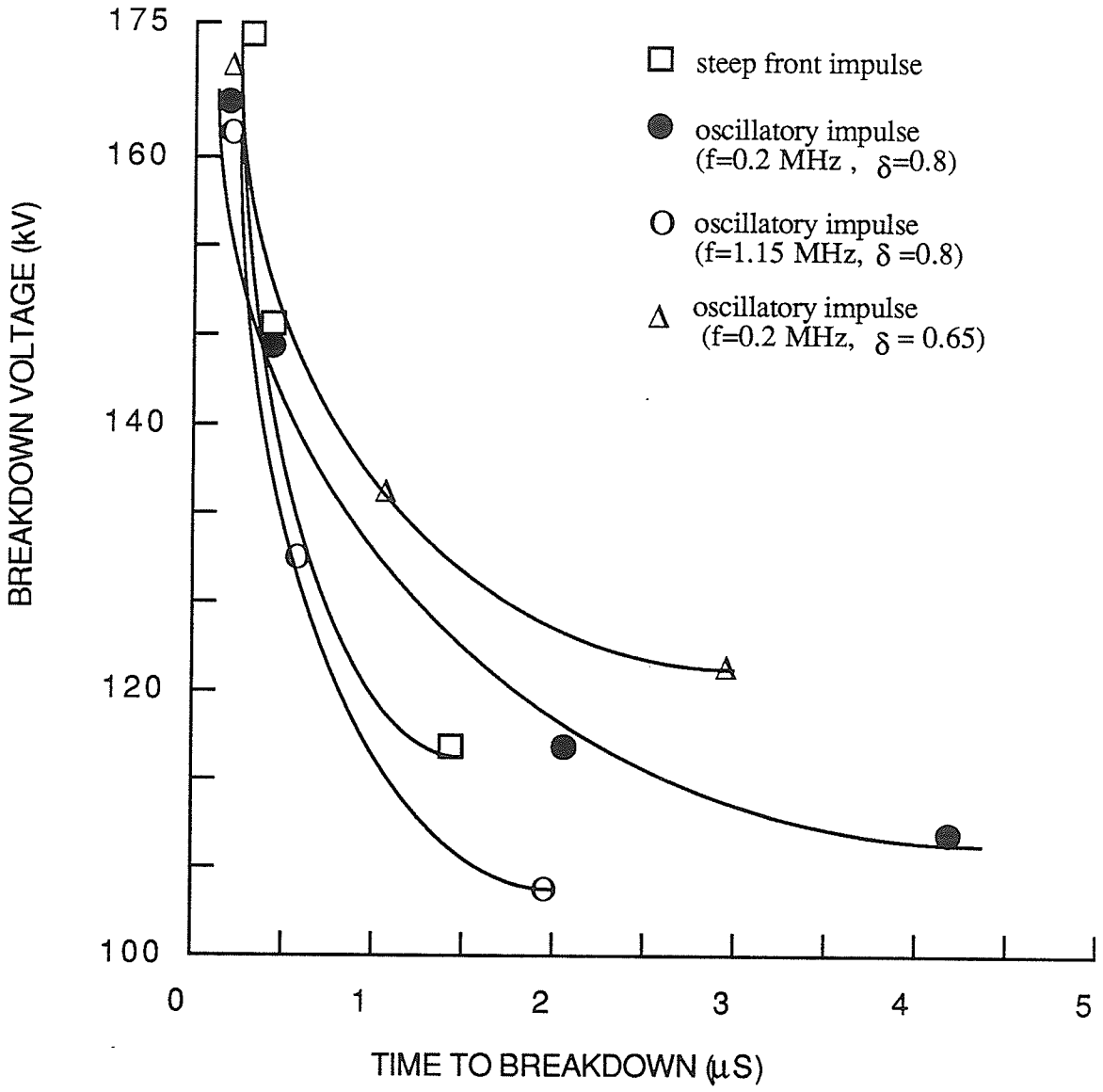


Figure 4.17: Surface strength Volt-time characteristics of processed pressboard under steep front impulse and oscillatory cos-bidirectional impulses with different frequencies and damping factor: 5 mm gap

of oscillatory impulse has little effect on the dielectric strength . Such behavior was also noted in [20] and [21] with rod/sphere oil gaps with different gap lengths from 5 to 15 mm. The data in Table 4.1 show that the 50 % surface breakdown voltages of processed pressboard with aged oil are approximately 25 % and 32 % lower than that obtained with new oil under steep front and oscillatory impulses respectively ; it also need to note that the 50 % breakdown voltage with aged oil under steep front impulse is approximately 13 % lower than

TABLE 4.1

The 50% surface breakdown voltages of processed pressboard

| Gap length | Oil type | Impulse type | 50% breakdown voltage (kV) |
|---|---|---|---|
| 5 mm | New oil | lightning | 100.5 |
| | | steep front | 116.4 |
| | | oscillatory 1 | 109.2 |
| | | oscillatory 2 | 123.5 |
| | | oscillatory 3 | 104.8 |
| | Aged oil | steep front | 87.5 |
| | | oscillatory 1 | 74.5 |
| 10mm | New oil | lightning | 170.2 |
| | | steep | 183.1 |

oscillatory 1: oscillatory impulse with f=0.2 MHz and $\delta$ =0.8
oscillatory 2: oscillatory impulse with f=0.2 MHz and $\delta$ =0.65
oscillatory 3: oscillatory impulse with f=1.15 MHz and $\delta$=0.8

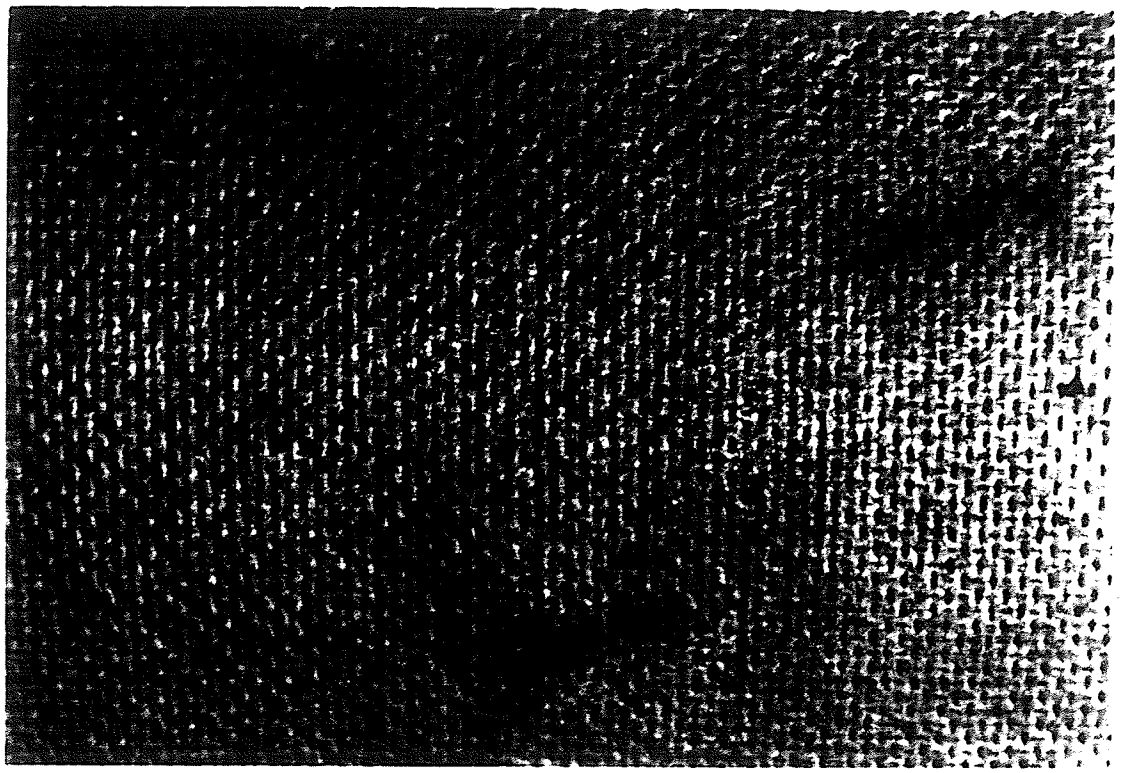

Figure 4.18: Surface tracks following surface breakdown under steep front impulse; 10 mm gap: tracked gap on the left broke down at 232.6 kV; tracked gap in the middle breakdown at 212.7 kV; tracked gap on the right broke down at 239.4 kV

that with fresh oil under standard lightning impulse. These phenomena indicate that the reliability of power transformer could be affected by aged oil.

The experimental data also showed that most breakdowns occurred in the interelectrode space and not on the surface of the pressboard when chopping occurred on the tail of the impulse voltage. Under these conditions, the same gap was used in further tests after thorough degassing. When the same gap was used in subsequent tests, it was found that the second and subsequent breakdowns occurred at different locations and no abnormalities were noted. In contrast, most breakdowns occurred on the surface of the pressboard when chopping occurred close to the crest. Even in these cases, it was found that the same test gap could be used for further testing, no reduction of breakdown voltages were observed if the system was completely degassed and the second and subsequent breakdowns did not occur at the same position. However this was not done because of the long time required to degas the specimen.

It was also found that the breakdowns on the surface of processed pressboard under oscillatory impulse with a lower damping factor ( $\delta$=0.65 ) caused the most damage followed by oscillatory impulses with frequency f = 0.2 MHz, oscillatory impulse with frequency f = 1.15 MHz, steep front impulse and lightning impulse. There were no breakdowns on the surface with aged oil under both steep front and oscillatory impulse voltages.

Figure 4.18 illustrate the damaged surface under steep front impulse.In this Figure, three tracks are visible ; these correspond to three 10 mm gaps; the gap on the left broke down at 232.6 kV, the gap in the middle broke down at 212.7 kV and the gap on the right broke down at 239.4 kV.

# CHAPTER 5

# THEORETICAL EXPLANATIONS AND DISCUSSIONS

## 5.1 Volt-time Area Law Theory

The reduction of surface breakdown strength under steep front impulses can be possibly explained by two different theories ; the volt-time area law and the sweeping action theory.

The volt-time area law was generally accepted by many authors [ 19, 20, 31, 32 ] to estimate the volt - time characteristics of fast rising impulse. These authors considered these characteristics from the point of view of the statistical and formative time lags. The breakdown time lag $t_c$ is considered to be composed of three parts as shown in Figure 5.1 and equation (5.1).

$$t_c = t_0 + t_s + t_f \qquad (5.1)$$

where $t_0$ is the time to reach the minimum breakdown voltage $V_0$ ; $t_s$ is the time lag for an initial electron to appear ( statistical time lag ) ; and $t_f$ is the time lag for breakdown formation ( formative time lag ).

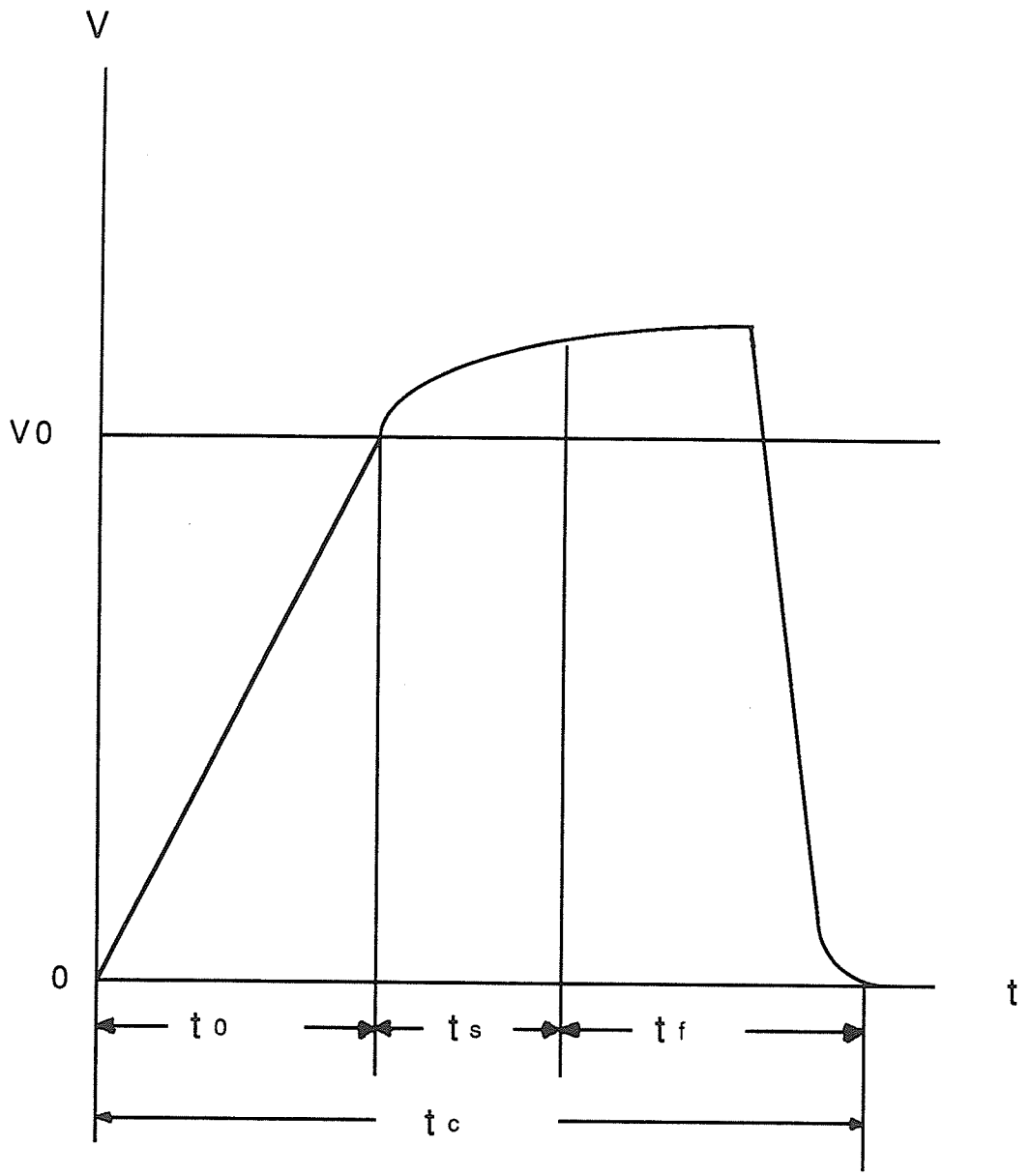


$V_0$: minimum breakdown voltage

$t_c$: total time lag

$t_0$: time to reach $V_0$

$t_s$: statistical time lag

$t_f$: formative time lag

Figure 5.1: Time lag in breakdown

The lower limiting curve of the volt-time characteristics will be obtained under the condition $t_s = 0$ ( $t_c = t_0 + t_f$ ). The voltage-time area law postulates that [33].

$$\int_{t_0}^{t_0+t_f} \{V(t) - V_0\}\, dt = A_f = \text{constant.} \qquad (5.2)$$

where $A_f$ is the voltage-time area as showing in Figure 5.2.

For considering both statistical time lag $t_s$ and formative time lag $t_f$ an "extended equal area law" has been proposed [ 33]

$$\int_{t_0}^{t_0+t_s+t_f} \{V(t) - V_0\}\, dt = A_s + A_f = \text{constant.} \qquad (5.3)$$

Using the volt - time area law, we can easily explain the decrease of surface breakdown value with increasing breakdown time which was found in our study. As illustrated in Figure 5.2, when the breakdown time increases from $t_1$ to $t_2$, the surface strength has to decrease from $v_1$ to $v_2$ because of the equality of shaded areas demanded by the volt-time area law.

It is difficult to explain quantitatively the reduction in breakdown strength when steep front impulses are applied, but the phenomenon could still be possibly explained by means of the volt - time area law. As can be seen in Figure 5.3 , the front slope of impulse voltage V1 (t) is steeper than that of impulse voltage V2 (t) : However it is possible for both the breakdown voltage V1 and breakdown time t1 under impulse V1 (t) to be less than V2 and t2

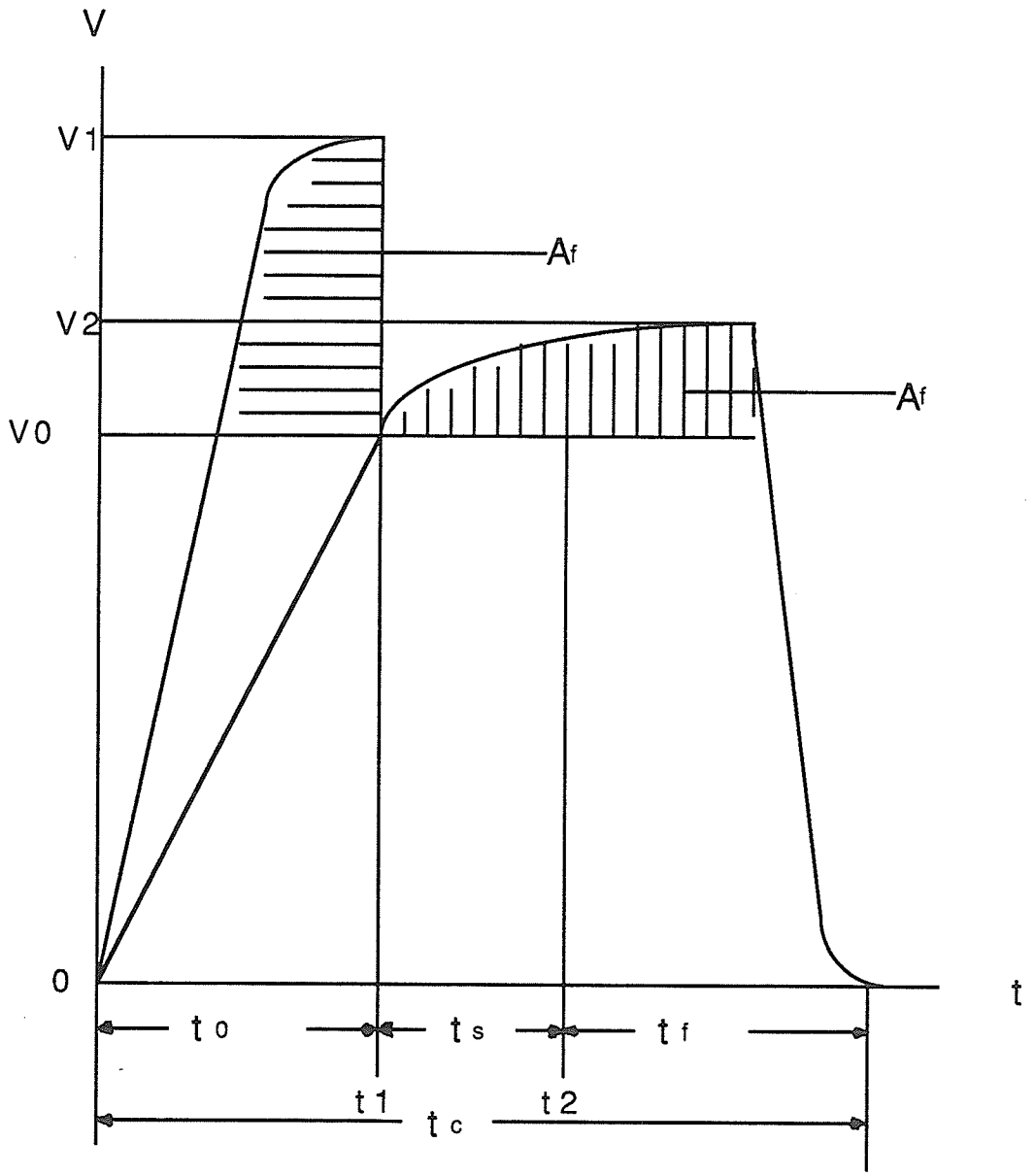


Figure 5.2 : Voltage-time law for breakdown formation time lag

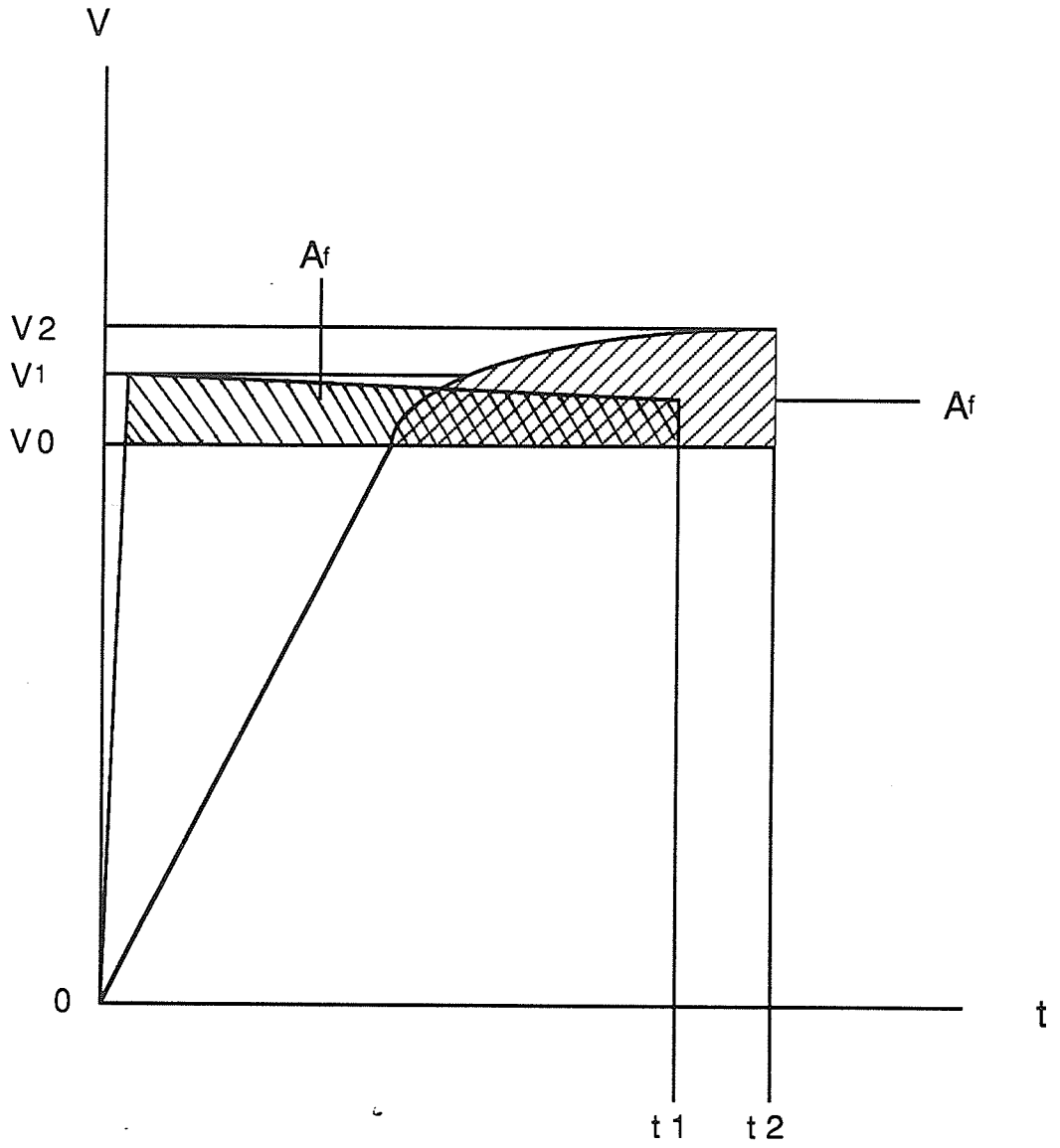


Figure 5.3: volt-time area law for steep front impulse and lightning impulse

( under impulse V2 (t) ) . In this case , as shown in Figure 5.3 , the shaded volt-time areas are equal under both impulse voltages . Although the volt - time area law is frequently used to evaluate the voltage-time characteristics, it is not accepted by some authors [18, 34-35] . These authors argue that the assumptions in the volt-time law may not be always applicable , because the average number of electrons in the gap is not constant but increases with the overvoltage ratio. Thus another theory called "sweeping action effect " introduced by Meek [34] is used to explain the abnormal behaviors under steep front impulses.

## 5.2 "Sweeping action" effect

The " sweeping action " effect reported in several papers [18,34-35] may be used to explain the reduction in breakdown strength when steep front impulses are applied. This theory states that under slowly rising impulses, most electrons are swept out of the critical region or out of the gap before the applied voltage reaches inception level . This causes an increase of the statistical time lag and therefore will increase the average breakdown voltage . Under fast rising impulses, the applied voltage may reach the inception level before the electrons are removed from the critical region, leading to shorter statistical time lag and possibly to the reduction of the average breakdown voltage.

In an publication, Meek [ 34] reported a decrease of impulse ratio for small sphere gaps in air with increasing front steepness in the the impulse. He attributed the effect to the " sweeping action " of electrons. In his explanation

he argued that under slowly rising impulses , the electrons are swept out of the gap before the voltage reaches a value high enough to initiate breakdown. Under steeply rising impulses , the voltage may reach a level high enough to initiate avalanche formation before the electrons are removed from the gap.Recently Qiu [ 35 ] reported low impulse ratios for enclosed gaps under steep front impulses. The reported difference between standard impulses and steep front ones was even larger than the earlier data reported by Meek. The " sweeping action " explanation is also consistent with the observed decrease in scatter reported in Qiu's paper.

As the mechanism of the breakdown under fast rising impulses is yet to be fully understood, satisfactory explanations can not be given at present. In the author's opinion, both the voltage-time law and sweeping action theory may be used to explain qualitatively the abnormal phenomenon under steep front impulses.

# CHAPTER 6

# CONCLUSIONS

The surface breakdown strength of cylindrical processed pressboard samples were studied experimentally under standard lightning, steep front and high frequency oscillatory impulses using both fresh mineral oil and aged mineral oil. Both 5 mm and 10 mm gaps have been investigated . The investigation focussed on the surface breakdown volt-time characteristics under lightning impulse and steep front impulse with a front duration as low as 0.15 μs .The influence of frequency and damping factor of oscillatory impulses were also studied using the same test configurations.

From the discussion included in previous chapters the following conclusions are drawn:

The experimental results show that the volt-time characteristics of surface breakdown strength for the 10 mm surface gap under lightning impulse and steep front impulse are discontinuous. An apparent reduction of the surface strength under steep front impulses is observed with both the 5 mm and 10 mm gaps.This

phenomenon could be qualitatively explained by considering the volt-time area law or sweeping action theory.

With damped oscillation impulses, it was found that the volt-time surface breakdown strength is greatest with the frequency $f = 0.2$ MHz and damping factor $\delta = 0.65$ followed by waveform with $f = 0.2$ MHz & $\delta = 0.8$ and $f = 1.15$ MHz & $\delta = 0.8$ for the 5 mm gap length. It is interesting to note that the frequency of the high frequency oscillatory impulses has little effect on the 50 % surface breakdown strength of processed pressboard. In this case, the breakdown strength under high frequency impulses with damping factor $\delta = 0.8$ is almost the same as that under lightning impulse. However, the damping factor has a significant influence on the breakdown voltages.

These studies also reveal that the 50 % surface strength is reduced by 25 % and 32 % in aged oil under steep front and oscillatory impulses respectively. The slope of the volt-time curves are steeper in aged oil than that in new oil. These results indicate that the electrical stress of serviced transformers decreased with the increase of operating hour.

It was also found that the breakdowns usually occurred on the surface of the pressboard when chopping was close to the crest . When chopping occurred on the tail of the impulse , breakdowns usually occurred in the interelectrode space . The impulse breakdown voltages were higher when breakdown occurred on the surface of the processed pressboard.

The oscillatory impulse with a lower damping factor ( $\delta = 0.65$ ) caused more damage on the surface of processed pressboard than any other impulse. Steep front impulses caused less damage than oscillatory impulses but more damage than lightning impulses . No breakdown on the surface in the aged

oil was observed under both steep front and oscillatory impulse voltages. In all cases, the damaged pressboard surface neither causes a reduction in the surface breakdown strength nor does it influence the location of subsequent breakdown if the sample is thoroughly degassed following breakdown.

In order to make a complete evaluation of the surface strength of processed pressboard , the following future work is recommended:

As mentioned earlier, the mechanism of the anomalous breakdown under fast rising impulses is still not clear . Therefore, fundamental research on the processes of breakdown is needed to estimate quantitatively the volt-time characteristics. Furthermore, the surface strength characteristics under unidirectional oscillatory impulses and sinusoidal oscillatory impulses still need to be studied. Finally, the surface strength characteristics of flat processed pressboard under steep front and oscillatory impulses should also be investigated.

# REFERENCES


1. Y. Kamata and Y. Kako, " Flashover Characteristics of Extremely Long Gaps in Transformer Oil under Non-uniform Field Conditions ", IEEE Transactions on Electrical Insulation, Vol. EI-15, No.1, Dec. 1980, pp. 18-22.

2. W. G. Standring and R. C. Hughes, " Breakdown under Impulse Voltages of Solid and Liquid Dielectrics in Combination ", Proc. IEE, Vol. 103 A, pp. 583-597, 1956.

3. W. G. Standring and R. C. Hughes , " Impulse Breakdown Characteristics of Solid and Liquid Dielectrics in Combination " , Proc. IEE. Vol. 109 A, pp. 473-488 , 1962.

4. K. Wechsler and M. Riccitiello, " Electrical Breakdown of A Parallel Solid and Liquid Dielectric System, " Trans. AIEE, Vol. 80, pp. 365-369, 1 961.

5. G. Maier and H. J. Vorwerk, " Dielectric Strength of Oil Impregnated Insulation under HVDC Stress " , Brown Boveri Review, No.5, pp 246-255, 1969.

6. E. F. Kelley and R. E. Hebner , Jr. , " Electrical Breakdown in Composite

Insulation Systems : Liquid - solid Interface Parallel to the Field " , IEEE Transactions on Electrical Insulation, Vol. EI-16, pp. 297-303, August 1981.

7. M. U. Anker , " Effect of Test Geometry , Permitivity Matching and Metal Particles on the Flashover Voltage of Oil / Solid Interfaces " , presented at IEEE PES Summer Meeting , Los Angeles, CA, No. 83 SM 436-3, July 17-22, 1983.

8. Z. Kolaczkowski , M. R. Raghuveer , S. Grzybowski and E. Kuffel , " Lightning and Switching Impulse Surface Strength of Processed Pressboard " , Sixth International Symposium on High Voltage Engineering, 13.10 , New Orleans, 1989.

9. S. Grzybowski and E. Kuffel, " Electrical Breakdown Strength of Polypropylene Film Oil Immersed under Combined ac-dc Voltage ", 1986 Conference on Electrical Insulation and Dielectric Phenomenon, Delaware.

10. H. Nowaczyk, S. Grzybowski, E. Kuffel, " Influence of Voltage Prestressing on the Dielectric Strength of Paper Oil Insulation , " IEEE Transactions on Electrical Insulation, Vol. EI-22, 1982, p.249

11. Jin Wei Fang , M. R. Raghuveer, J. Gzylewski and E. Kuffel, " Behavior of Impregnated Composite Insulation under High Voltage at Very Low Frequency ", IEEE Transactions on PAS, Vol. PAS-101, No.9, September 1982, pp. 3158-3165.

12. " Report on Experimental determination of the Electrical Surface Strength of Pressboard in Mineral Oil under dc Voltage with Ripple", Research Report, High Voltage Lab. University of Manitoba, 1989.

13. S. R. Naidu, J. B. Neison and K. D. Srivastava," The Voltage-time Characteristics of Oil-impregnated Paper Insulation in the Submicrosecond and Microsecond Regime", IEEE Transactions on Electrical Insulation, Vol. EI-24, No.1, February 1989, pp. 39-46.

14. L. M. Burrage, P. F. Hettwer and B. W. McConnell, " Impact of Steep Front Short Duration Impulses on Power System Apparatus and Insulation : A Critical Eeview ", IEEE Int'l Symp. on Electrical Insulation , Washington DC, Paper D-5, June 6-11, 1986.

15. M. R. Raghuveer, " A Research Proposal for Surface Strength of Transformer Insulation under Steep Front Voltages ", Oct. 15,1987.

16. R. E. Clayton, I. S. Grant, D. E. Hedman and D. D. Wilson , " Surge Arrester Protection and Very Fast Surges ", IEEE Transactions on Power Apparatus and Systems , Vol. PAS-102, No.8, August 1983, pp. 2400-2406.

17. M. Nagano, S. Masuda, M. Nara and H. Inoue ," Measurements of Steep Front Lightning Surge Voltages on Distribution Lines " , IEEE Transactions on Power Apparatus and Systems , Vol. PAS-102, No.6 , June 1983 pp.1598-1602.

18. Ziqin Li , R. Kuffel and E. Kuffel , " Voltage-time Characteristics in Air, SF6 / Air Mixture and N2 for Coaxial Cylinder and Rod-sphere Gaps", IEEE Transactions on Electrical Insulation , Vol. EI-21, No.2 , Apr. 1986, pp. 151-155.

19. F. A. M. Risk and M. B. Eteiba, " Impulse Breakdown Voltage- Time Curves of SF6 and SF6-N2, Coaxial Gaps ", IEEE Transaction on Power Apparatus and Systems , PAS, Vol. 101, pp. 4460-4468.

20. S. R. Naidu, Paulo de Tarso Mederos and K. D. Srivastava," Volt-Time Curves for Coaxial Cylindrical Gap in SF6 - N2 Mixtures ", IEEE Transactions on Electrical Insulation .Vol. EI-22 No.6, Dec. 1987 pp.755-761.

21. R. C. Degeneff , " Transformer Response to System Switching Voltage", IEEE PES Summer Meeting, Vol. 81, SM 319-3, 1981.

22. Tsuneharu Teranishi, Toshiyuki Yaanari, Masaki Honda and Tamotsu Inoue, " Dielectric Strength of Transformer Insulation Against Oscillatory Impulse Voltage ", Electrical Engineering in Japan, Vol. 104b, No.1, Jan. 1984, pp.57-63.

23. D. Breitfelder, E. Buckow, W. Knorr and W. Peschke, " Dielectric Strength of Transformer oil under Impulse and High Frequency Voltage Stress ", Fifth International Symposium on High Voltage Engineering, 22.12, Braunschweig, Aug.1987

24. Guan Zhicheng and I. D. Couper, " The Effect of Decaying Oscillatory Switching Waveforms on the Breakdown of Rod / Sphere Gaps ", Sixth International Symposium on High Voltage Engineering, 13.01, New Orleans, 1989.

25. R. J. Musil, G. Preininger , E. Schopper and S. Wenger , " Voltage Stresses Produced By Aperiodic and Oscillating system Overvoltages in transformer windings ", IEEE Transactions on Power Apparatus and systems, Vol. PAS-100, No. 1, Jan. 1981 pp.431-438.

26 Hideo Hirose, " A Method to Estimate the Lifetime of Solid Electrical Insulation " IEEE Transaction on Electrical Insulation Vol. EI-22 No.6 , Dec.

1987, pp. 745-753.

27. J. Gzylewski, Z. Makowski,"Suszenie Prozniowe Kondensatorow Energetycznych," Przeg Elektrot , RXL VIII 210, 1972, pp. 477.

28. Ziqin Li, " The Breakdown Voltage-Time Characteristics of SF6 and Its Mixtures in Coaxial Cylinder Gaps with Special Reference to Steep-fronted Impulse Voltages with Time to Chopping Down to 100 ns ", Thesis , University of Manitoba, 1989

29. IEEE Std 4-1978, pp.80-83.

30. S. Okabe and E. Kuffel, " Volt-time Characteristics of Rod - sphere Gaps in Mixtures Comprising SF6, c-C4F8, CO and Dry Air , SF6 ". Conf. Record of the 1984 . IEEE Inter. Symp. on Elect. Insul. pp. 143-146.

31 T. Yamagiwa and J. Ozawa, " Generalization of Equal Voltage-time Area Criterion for Estimating Voltage-time Characteristics of Various Arrangements in SF6 Gas. IEEE Transactions on Power Apparatus and systems, No. 4, April 1985 pp.764-767.

32 W. Taschner, " Dependence of Voltage-time Curves on the Front Steepness of Testing Voltage in SF6 , Measuring Method and Definitions ", CIGRE SC-15 , WG-03 , 1980

33 W. Knorr, " Voltage-time Characteristics of Slightly Non-uniform Arrangement in SF6 Using Linearly Rising and Oscillating Lightning Impulse voltages", CIGRE Paper 15 -05 , 1979

34 J. M. Meek, " The Influence of Irradiation on the Measurement of Impulse Voltages with Sphere Gaps ", IEE Journal, Vol. 93, Pt. II, p.97, 1946

35 Y. Qiu, " Impulse Breakdown Characteristics of Enclosed Sphere Gaps ", 4th International Symposium on High Voltage Engineering, Athens, Sept. 1983, Paper 33.07